iScience

CellPress
OPEN ACCESS

Article

T cell death-associated gene 8-mediated distinct signaling pathways modulate the early and late phases of neuropathic pain

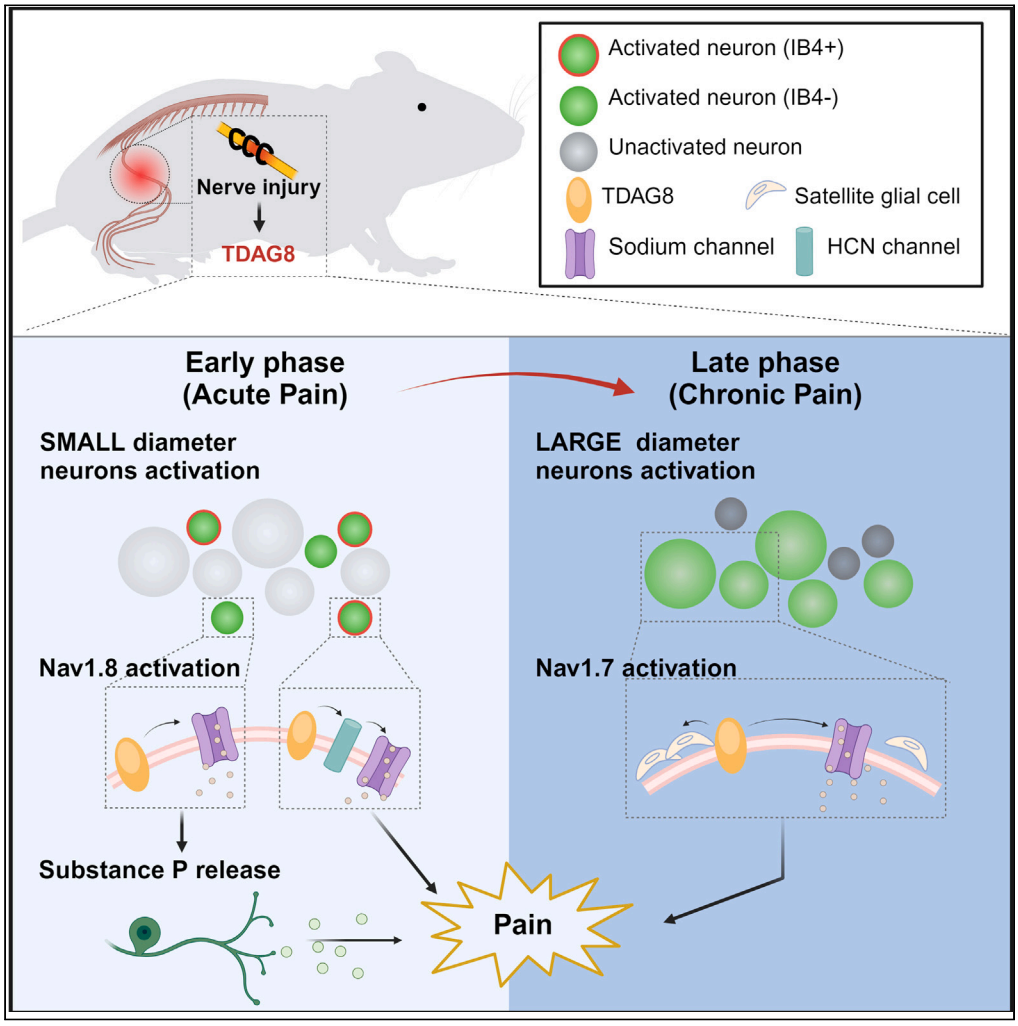

Shih-Ping Dai, Chun-Chieh Yang, Yin Chin, Wei-Hsin Sun

weihsin@nycu.edu.tw

Highlights

TDAG8-HCN-$Na_v1.8$ signaling in small IB4(+) neurons initiates mechanical allodynia

TDAG8 activation in small IB4(−) neurons releases SP to promote early mechanical allodynia

TDAG8 activation in large IB4(−) neurons increases SGC to maintain late mechanical allodynia

SP anti-nociceptive effects in soma prevent the development of late mechanical allodynia

Dai et al., iScience *27*, 110955
October 18, 2024
https://doi.org/10.1016/j.isci.2024.110955

iScience

CellPress
OPEN ACCESS

Article

T cell death-associated gene 8-mediated distinct signaling pathways modulate the early and late phases of neuropathic pain

Shih-Ping Dai,[1,3] Chun-Chieh Yang,[1,2,3] Yin Chin,[1] and Wei-Hsin Sun[1,2,4,*]

SUMMARY

Peripheral nerve injury alters the transduction of nociceptive signaling. The coordination of neurons, glia, and immune cells results in persistent pain and inflammation. T cell death-associated gene 8 (TDAG8), located at nociceptors and immune cells, is involved in inflammatory pain and arthritis-induced pain. Here, we employed TDAG8-deficient mice, pharmacological approaches, and calcium/sodium imaging to elucidate how TDAG8-mediated signaling modulates neuron activities in a mouse model of chronic constriction injury-induced neuropathic pain. We demonstrated that TDAG8 participated alone in mechanical allodynia induced by constriction injury. (1) TDAG8-$Na_v1.8$ signaling in small-diameter isolectin B4-positive [IB4(+)] neurons initiates mechanical allodynia; it also modulated substance P release from IB4(−) neurons to facilitate the development of early mechanical allodynia. (2) TDAG8-mediated signaling increased medium-to large-diameter IB4(−) neuron activity to maintain late mechanical allodynia; it also modulated substance P release in soma to reduce satellite glial number and $Na_v1.7$ expression, thus attenuating chronic mechanical allodynia.

INTRODUCTION

Neuropathic pain is a complex syndrome, resulting from damage due to trauma, compression, infection, and immune and metabolic diseases to the nervous system.[1] Neuronal injury profoundly alters the function of primary sensory neurons and their central pathways and is associated with a robust immune response, contributing to pain hypersensitivity to both thermal and mechanical stimuli as well as spontaneous pain.[2–5] Injured peripheral nerves release some mediators or peptides such as adenosine triphosphate (ATP), proton, substance P (SP), or calcitonin gene-related peptide (CGRP) to activate and recruit immune cells, which causes local tissue acidosis and inflammation.[6–8]

SP released from small-diameter isolectin B4-negative [IB4(−)] nociceptors transduces nociceptive signals. It can increase voltage-gated sodium channel 1.8 ($Na_v1.8$) expression and potentiate $Na_v1.8$ currents.[9,10] SP acts on the periphery to cause neurogenic inflammation, thus enhancing hypersensitivity.[11] SP could also act on A® non-nociceptive neurons, causing hypersensitivity.[12,13] In addition, SP has an anti-nociceptive role in inflammatory pain by regulating opioid release from central neurons or immune cells and muscle pain by activating the potassium channel (M channel) to cause hyperpolarization.[14]

SP also activates satellite glial cells (SGCs) to release mediators, which in turn increases neuron sensitivity or recruits more immune cells.[2–4,15,16] In a temporomandibular joint inflammation model, inhibition of SGC activation by a connexin 43 (a gap junction protein) blocker decreased the expression of $Na_v1.7$ and alleviated $Na_v1.7$-mediated mechanical hypernociception.[17]

Tissue acidosis activates acid-sensing receptors which sensitize peripheral nociceptors, thus triggering pain and hyperalgesia.[18–20] T cell death associated gene 8 (TDAG8) was identified as a proton-sensing G protein-coupled receptor (GPCR) with full activation at pH 6.4–6.8.[21,22] Approximately 68% of TDAG8 expression is located in small-diameter neurons and 47% in IB4(+) neurons.[6] TDAG8 regulates protein kinase A (PKA) signaling to initiate hyperalgesia and establish hyperalgesic priming in inflammatory pain models. Indeed, in complete Freund's adjuvant (CFA)-induced inflammation, TDAG8 deficiency in peripheral neurons inhibited the initial hyperalgesia (1–4 h) and shortened prolonged hyperalgesia.[23] Genetic deletion or pharmacological blockage of TDAG8 attenuated arthritis-induced chronic pain by reducing the number of SGCs.[15,24,25] Also, TDAG8 activation in microglial or immune cells seemed to inhibit the production of pro-inflammatory cytokines,[26–28] thereby reducing the inflammatory response. However, it remains unclear whether TDAG8 also plays a similar role in the neuropathic pain model and what the underlying mechanism is.

Here we investigated the role of TDAG8 in a mouse model of constriction-injury-dependent neuropathic pain and found that it is involved in mechanical allodynia but not thermal hyperalgesia induced by nerve injury. In early mechanical allodynia, TDAG8 activation modulated

[1]Department of Life Sciences and Institute of Genome Sciences, National Yang Ming Chiao Tung University, Taipei, Taiwan
[2]Program in Molecular Medicine, National Yang Ming Chiao Tung University and Academia Sinica, Taipei, Taiwan
[3]These authors contributed equally
[4]Lead contact
*Correspondence: weihsin@nycu.edu.tw
https://doi.org/10.1016/j.isci.2024.110955

$Na_v1.8$ in small-diameter IB4(+) neurons to initiate mechanical allodynia. TDAG8-mediated SP release from IB4(−) neurons in the periphery facilitated early mechanical allodynia. In late mechanical allodynia, TDAG8 activation modulated medium-to large-diameter IB4(−) neuron activity to lead to chronic mechanical allodynia. TDAG8-mediated SP release in soma reduced satellite glial number and downregulated $Na_v1.7$ expression, thus attenuating the chronic mechanical allodynia.

RESULTS

T cell death-associated gene 8 activation modulates both the early and late phases of mechanical allodynia

Previous studies have suggested that TDAG8 is involved in inflammatory pain.[23] To explore whether the proton-sensing receptor TDAG8 also participates in neuropathic pain, we first examined TDAG8 gene expression in DRG after CCI surgery and found that it was increased at weeks 1 and 2, decreased at week 3, then increased again at week 14 (Figure 1A). No TDAG8 gene expression was observed in $TDAG8^{-/-}$ mice at 2 and 14 weeks after CCI surgery (Figure 1B). Because TDAG8 activation mediates cAMP accumulation, we then examined whether the TDAG8-mediated cAMP signaling pathway was also inhibited in $TDAG8^{-/-}$ mice. At 2 or 14 weeks after CCI surgery, the intracellular cAMP level was accumulated in DRG in $TDAG8^{+/+}$ mice but blocked in $TDAG8^{-/-}$ mice (Figure 1C). The results confirmed that TDAG8 expression and function were inhibited after TDAG8 gene deletion.

We then examined pain-like behavior in $TDAG8^{+/+}$ or $TDAG8^{-/-}$ mice. Similar to observations in ICR mice in the previous study,[29] CCI induced long-term unilateral mechanical allodynia and thermal hyperalgesia in $TDAG8^{+/+}$ male mice (Figures 1D and 1E). Notably, TDAG8 gene deletion reduced mechanical allodynia in the early phase (1–4 weeks) and late phase (>13 weeks) in male mice (Figure 1D). TDAG8 deletion did not affect thermal hyperalgesia in male mice (Figure 1E). Female mice also exhibited similar results of TDAG8 deficiency: delayed onset of mechanical allodynia and shortened mechanical allodynia (Figure 1F). No differences in thermal hyperalgesia were observed between $TDAG8^{+/+}$ and $TDAG8^{-/-}$ female mice (Figure 1G). Hence, TDAG8 activation may regulate both the early and late phases of mechanical allodynia but not thermal hyperalgesia.

T cell death-associated gene 8 activation modulates <20-μm diameter isolectin B4-positive [IB4(+)] and IB4(−) neuron activity in early mechanical allodynia but regulates >20-μm diameter IB4(−) neuron activity in the late phase

As previously suggested,[30,31] TDAG8 activation by acidic buffer increased cAMP level and also $[Ca^{2+}]_i$ level. Thus, we used calcium imaging to examine whether TDAG8 was activated in nociceptors and whether early and late mechanical allodynia were controlled by TDAG8-expressing nociceptors. Approximately 64% of TDAG8 level was expressed in the IB4-positive non-peptidergic nociceptor.[3] After CCI, acid (pH 6.8)-induced calcium signals were increased at week 2 in $TDAG8^{+/+}$ IB4(+) DRG neurons, then decreased to basal levels at week 14 (Figure 2A). In $TDAG8^{+/+}$ IB4(−) DRG neurons, acid-induced calcium signals were increased at weeks 2 and 14 after CCI surgery (Figure 2B). TDAG8 deletion inhibited the increase at week 2 in IB4(+) neurons and at both weeks 2 and 14 in IB4(−) neurons (Figures 2C–2F). Approximately 89% of total $TDAG8^{+/+}$ DRG neurons responded to pH 6.8 stimulation [88% for IB4(+) and 90% for IB4(−) neurons], whereas TDAG8 deletion reduced pH 6.8-responding neuron number to 65% [60% in IB4(+) and 70% in IB4(−) neurons].

Increased calcium signals in IB4(+) neurons were mainly attributed to <20-μm diameter neurons at week 2 (Figure 2G). Increased calcium signals in IB4(−) neurons were attributed to <20-μm diameter neurons at week 2 but to >20-μm diameter neurons at week 14 (Figure 2H). By using the TDAG8 antagonist NSC745885, we confirmed that the increased calcium signals at 2 weeks after CCI was significantly inhibited in IB4(+) neurons and slightly decreased in IB4(−) neurons (Figures 2I and 2J). NSC745885 significantly reversed increased calcium signals at 14 weeks after CCI in IB4(−) neurons but not in IB4(+) neurons (Figures 2K and 2L). These data suggest that TDAG8 activation modulated IB4(+) and IB4(−) neuron activities in the early phase but regulated IB4(−) neuron activity in the late phase. Also, the major responsive neuron size was switched from <20-μm to >20-μm diameter. Accordingly, <20-μm IB4(+) neurons may be involved in only the early phase of mechanical allodynia; <20-μm diameter IB4(−) neurons likely participate in the early phase, and >20-μm diameter IB4(−) neurons in the late phase.

To distinguish the sub-population of IB4(−) neurons, we co-stained anti-TDAG8 antibody with anti-neurofilament (N52), anti-calcitonin gene-related peptide (CGRP) or IB4-FITC conjugates. We found that TDAG8 was mainly expressed in small DRG neurons before CCI (0w) in both IB4(+) and CGRP(+) neurons (Figure S1A), consistent with our previous study.[6] At 2 weeks after CCI, TDAG8 was expressed more in N52 (+), IB4 (+) and CGRP (+) neurons (Figure S1B). At 14 weeks after CCI, TDAG8 expression was increased mainly in N52(+) neurons, but less expressed in IB4(+) and CGRP(+) neurons (Figure S1C). These data were consistent with our calcium imaging data that TDAG8 response in small IB4(+) and IB4(−) neurons in the early phase while TDAG8 response shifted to large N52(+) neurons in the later phase (Figures 2E–2H).

To understand whether ASIC1a, ASIC3, TRPA1, and TRPV1 are involved in acid-induced calcium or sodium signals, DRG was taken 2w after CCI, cultured, followed by acid stimulation and calcium or sodium imaging. Antagonists for ASIC1a (PcTx1, Figures S2A and S2B), ASIC3 (APETx2, Figures S2C and S2D), TRPA1 (HC030031, Figures S2E and S2F), and TRPV1 (Capsazepine, Figures S2G and S2H) were used to examine the involvement of these channels. Acid-induced calcium or sodium signals were not inhibited by any antagonists used, suggesting that ASIC1a, ASIC3, TRPA1, and TRPV1 are not involved in acid-induced calcium or sodium signals in the early phase of neuropathic pain. We also examined TRPV1 expression in $TDAG8^{+/+}$ and $TDAG8^{-/-}$ DRGs and no significant change in TRPV1 gene expression was found after TDAG8 deletion (Figure S2I). No apparent alteration in CCI-induced mechanical allodynia between $TRPV1^{+/+}$ and $TRPV1^{-/-}$ male mice were found (Figure S2J), suggesting that TRPV1 is not involved CCI-induced mechanical allodynia. ASIC3 expression was up-regulated in $TDAG8^{+/+}$ DRG (Figure S2K). TDAG8 deletion did not significantly down-regulate ASIC3 expression (Figure S2K) despite the fact that ASIC3 is involved in the later phase of mechanical allodynia.[29]

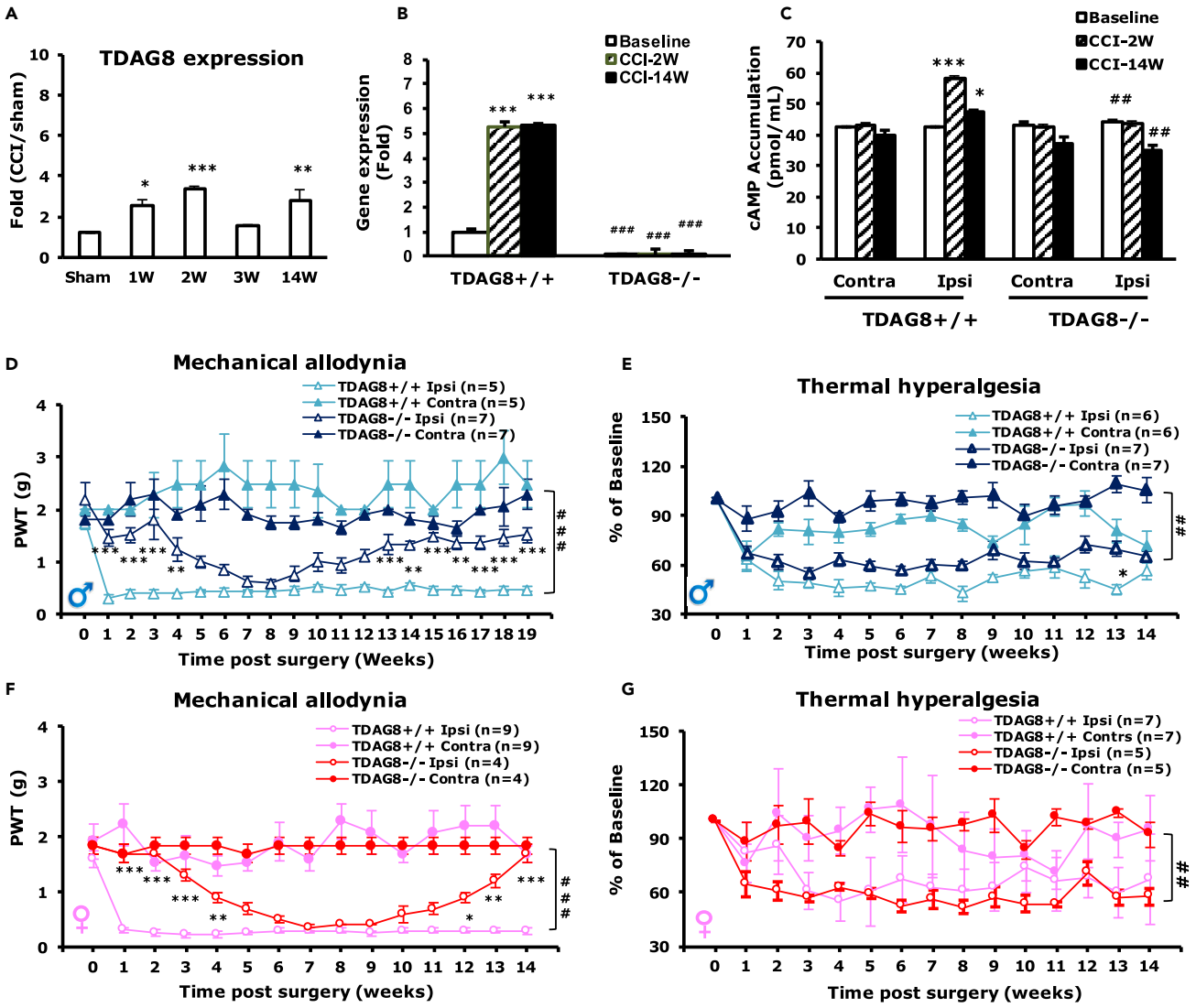

Figure 1. TDAG8 gene deletion reverses mechanical allodynia in both early and late phases

(A) RT-qPCR analysis of TDAG8 gene expression in L5 DRG from male mice with chronic constriction injury (CCI) of the sciatic nerve (n = 3 for each group) at 1, 2, 3, and 14 weeks. The sham control was at 1 week after CCI. Sham vs. 1w CCI *p = 0.039; Sham vs. 2w CCI ***p < 0.001; Sham vs. 14w CCI **p = 0.003 by one-way ANOVA with post-hoc Bonferroni test. Data are mean ± SEM.

(B–G) The sciatic nerve of mice with or without TDAG8 deletion was loosely ligated three times. (B) RT-qPCR analysis of TDAG8 gene expression in L4-6 DRG from $TDAG8^{+/+}$ or $TDAG8^{-/-}$ CCI male and female mice (n = 3 for each group) at 2, and 14 weeks. Baseline vs. $TDAG8^{+/+}$CCI-2W ***p < 0.001; Baseline vs. $TDAG8^{+/+}$CCI-14W ***p < 0.001; $TDAG8^{+/+}$ baseline vs. $TDAG8^{-/-}$ baseline ###p < 0.001; $TDAG8^{+/+}$ CCI-2w vs. $TDAG8^{-/-}$ CCI-2w ###p < 0.001; and $TDAG8^{+/+}$CCI-14w vs. $TDAG8^{-/-}$CCI-14w ###p < 0.001 by two-way ANOVA with post-hoc Bonferroni test. Data are mean ± SEM. (C) At 2 and 14 weeks after surgery or without surgery (baseline), L4-6 DRG were isolated and cAMP was detected by ELISA. Baseline vs. $TDAG8^{+/+}$CCI-2w ***p < 0.001; baseline vs. $TDAG8^{+/+}$CCI-14w *p = 0.037; $TDAG8^{+/+}$ CCI-2w vs. $TDAG8^{-/-}$ CCI-2w ##p = 0.004; $TDAG8^{+/+}$ CCI-14w vs. $TDAG8^{-/-}$ CCI-14w ##p = 0.005 by two-way ANOVA. N = 3 male and female mice for each group. Data are mean ± SEM. (D–G) Behavioral tests were performed in male (D, E) or female mice (F, G) for mechanical stimuli (D, F) or thermal stimuli (E, G) before (0 weeks) or after (1–19 weeks) surgery. Data are mean ± SEM; *p < 0.05; **p < 0.01, ***p < 0.001 for $TDAG8^{+/+}$ vs. $TDAG8^{-/-}$; #p < 0.05; ##p < 0.01, ###p < 0.001 for 0 weeks vs. other weeks by two-way ANOVA with post-hoc Bonferroni test. N = 4–9. (D) $TDAG8^{+/+}$ Ipsi 0w vs. other weeks p < 0.001; $TDAG8^{-/-}$ Ipsi vs. $TDAG8^{+/+}$ Ipsi at 1, 2, 3, 13, 15, 17, 18 or 19w p < 0.001; at 4w p = 0.008; 14w p = 0.007; 16w p = 0.007. (E) $TDAG8^{+/+}$ Ipsi 0w vs. other weeks p < 0.01; $TDAG8^{-/-}$ Ipsi vs. $TDAG8^{+/+}$ Ipsi at 13w p = 0.021. (F) $TDAG8^{+/+}$ Ipsi 0w vs. other weeks p < 0.001; $TDAG8^{-/-}$ Ipsi vs. $TDAG8^{+/+}$ Ipsi at 1, 2, 3 and 14w p < 0.001; at 4w p = 0.006; 12w p = 0.029; 13w p = 0.007. (G) $TDAG8^{+/+}$ Ipsi 0w vs. other weeks p < 0.01.

T cell death-associated gene 8 activation regulates $Na_v1.8$ gene expression and function in the early chronic constriction injury phase

Both $Na_v1.7$ and $Na_v1.8$ are major voltage-gated sodium channels expressed in DRG neurons. To understand whether TDAG8 activation modulates voltage-gated sodium channels to affect the early and late phases of mechanical allodynia, we examined $Na_v1.7$ and $Na_v1.8$

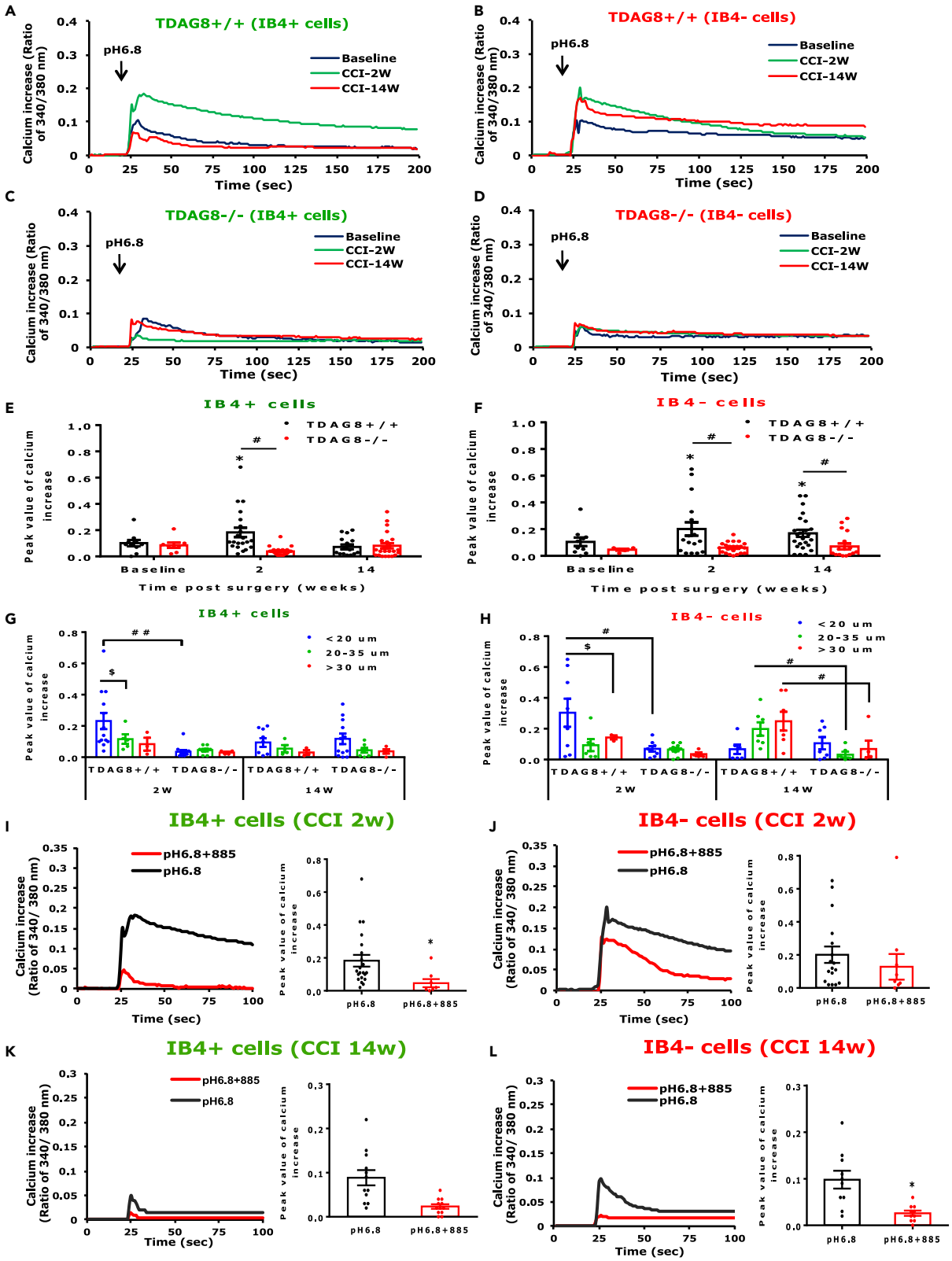
A
TDAG8+/+ (IB4+ cells)
pH6.8
Baseline
CCI-2W
CCI-14W
Calcium increase (Ratio of 340/380 nm)
Time (sec)
B
TDAG8+/+ (IB4- cells)
C
TDAG8-/- (IB4+ cells)
D
TDAG8-/- (IB4- cells)
E
IB4+ cells
TDAG8+/+
TDAG8-/-
Peak value of calcium increase
Baseline
2
14
Time post surgery (weeks)
F
IB4- cells
G
IB4+ cells
< 20 um
20-35 um
> 30 um
TDAG8+/+
TDAG8-/-
2W
14W
H
IB4- cells
I
IB4+ cells (CCI 2w)
pH6.8+885
pH6.8
Calcium increase (Ratio of 340/ 380 nm)
J
IB4- cells (CCI 2w)
K
IB4+ cells (CCI 14w)
L
IB4- cells (CCI 14w)

Figure 2. Calcium signals are increased at 2 and 14 weeks after CCI surgery and inhibited by TDAG8 gene deficiency

(A–H) Ipsilateral L4-6 DRG were taken from TDAG8$^{+/+}$ or TDAG8$^{-/-}$ male and female mice before (baseline) or at 2 and 14 weeks after CCI surgery, then intracellular calcium signals were detected in cultured DRG neurons. After detection, neurons were stained with IB4-FITC conjugates to distinguish IB4(+) and (−) neurons. (A–D) The time course of intracellular calcium signals is shown in A, B for TDAG8$^{+/+}$ DRG and C, D for TDAG8$^{-/-}$ DRG. (E, F) Mean ± SEM peak values for calcium signals in total neurons. (E) TDAG8$^{+/+}$ baseline vs. TDAG8$^{+/+}$ CCI-2w *p = 0.039; TDAG8$^{+/+}$ CCI-2w vs. TDAG8$^{-/-}$ CCI-2w #p = 0.031 by one-way ANOVA with a post-hoc Bonferroni test. (F) TDAG8$^{+/+}$ baseline vs. TDAG8$^{+/+}$ CCI-2w *p = 0.027; TDAG8$^{+/+}$ baseline vs. TDAG8$^{+/+}$ CCI-14w *p = 0.041; TDAG8$^{+/+}$ CCI-2w vs. TDAG8$^{-/-}$ CCI-2w #p = 0.039, TDAG8$^{+/+}$ CCI-14w vs. TDAG8$^{-/-}$ CCI-14w #p = 0.043 by one-way ANOVA with a post-hoc Bonferroni test. (G, H) Peak values for calcium signals in different populations of neurons. (G) < 20 μm TDAG8$^{+/+}$ CCI-2w, vs. 20–35 μm TDAG8$^{+/+}$ CCI-2w p = 0.032; <20 μm TDAG8$^{+/+}$ CCI-2w vs. <20 μm TDAG8$^{-/-}$ CCI-2w p = 0.002 by one-way ANOVA with a post-hoc Bonferroni test. (H) < 20 μm TDAG8$^{+/+}$ CCI-2w vs. >35 μm TDAG8$^{+/+}$ CCI-2w p = 0.039; <20 μm TDAG8$^{+/+}$ CCI-2w vs. TDAG8$^{-/-}$ <20 μm CCI 2w p = 0.030; 20–35 μm TDAG8$^{+/+}$ CCI-14w vs. 20–35 μm TDAG8$^{-/-}$ CCI-14w p = 0.021, >35 μm TDAG8$^{+/+}$ CCI-14w vs. >35 μm TDAG8$^{-/-}$ CCI-14w p = 0.041 by one-way ANOVA with a post-hoc Bonferroni test. (I–K) Ipsilateral L4-6 DRG were taken from TDAG8$^{+/+}$ male and female mice at 2 or 14 weeks after CCI surgery and cultured, then treated with pH 6.8 or pH 6.8+NSC745885 (885, TDAG8 antagonist). The time course of intracellular calcium signals is shown in the left panels of I, J, K, and L; the peak value for calcium signals is shown in the right panels. (I) pH 6.8 vs. pH 6.8 + 885 p = 0.038; (L) pH 6.8 vs. pH 6.8 + 885 p = 0.026 by unpaired t test. Significant symbols used in figures are defined as such: *p < 0.05, #p < 0.05, ##p < 0.01, $$p$ < 0.05.

gene expression in TDAG8-deficient mice. The expression of $Na_v1.8$ but not $Na_v1.7$ was increased at week 2 after CCI (Figures 3A and 3B). The increase in $Na_v1.8$ expression was inhibited by TDAG8 deletion (Figures 3A and 3B), so $Na_v1.8$ upregulation in the early phase of CCI was regulated by a TDAG8-mediated signaling pathway. To examine whether the $Na_v1.7$ and $Na_v1.8$ channels are involved in the mechanical allodynia, we first examined the time courses of $Na_v1.8$ channel selective antagonist A803467 and tetrodotoxin (TTX). A803467 or TTX was intraplantarly injected into mice at week 2 or 14 after CCI, respectively. It was found that the peak of A803467-induced inhibitory effect at 3 h after injection (Figure 3C) and the peak of TTX-induced inhibitory effect at 4–5 h after injection (Figure 3D). The time points of 3 h for A803467 and 4 h for TTX were used for further analysis.

We then intraplantarly injected A803467 into CCI mice at weeks 1, 2, or 3. Mechanical allodynia was reversed at weeks 1 and 2 but not in week 3 (Figure 3E). The administration of tetrodotoxin (TTX) at week 2 did not reverse the CCI-induced mechanical allodynia (Figure 3E), which suggests that $Na_v1.8$ is mainly involved in the early phase (1–2 weeks) of mechanical allodynia.

To further understand whether TDAG8 activation also regulates $Na_v1.8$ function in the early phase of CCI, we used sodium imaging to examine acid-induced sodium signals. Acid-induced sodium signals were significantly increased at week 2 in IB4(+) neurons in TDAG8$^{+/+}$ mice, whereas TDAG8 deletion inhibited acid-induced sodium signals at week 2 (Figures 3F, 3H, and 3J). Acid-induced sodium signals were only slightly increased in IB4(−) neurons, but this increase was also inhibited in TDAG8$^{-/-}$ mice (Figures 3G, 3I, and 3K). $Na_v1.8$ blocker (A803467) treatment revealed that acid-increased sodium signals were also inhibited in both IB4(+) and IB4(−) neurons (Figures 3F–3K), similar to the results obtained from TDAG8$^{-/-}$ mice. Acid-increased sodium signals were mainly attributed to <20-μm and 20- to 35-μm diameter neurons in IB4(+) neurons but to <20-μm diameter neurons in IB4(−) neurons (Figures 3L and 3M). Both TDAG8 deletion and $Na_v1.8$ blocker treatment inhibited the increased sodium signals in <20-μm diameter neurons (Figures 3L and 3M), which suggests that <20-μm diameter neurons are responsible for the early phase of mechanical allodynia.

In <20-μm diameter neurons, acid-induced sodium signals can be divided into four groups (I, II, III, IV) (Figure 3N). In group I, acid-induced sodium signals were inhibited by TDAG8-antagonist (NSC745885) and $Na_v1.8$-blocker (A803467) treatment. In group II, acid-induced sodium signals were inhibited by TDAG8-antagonist (NSC745885) but not $Na_v1.8$-blocker (A803467) treatment. In Group III, acid-induced sodium signals were not inhibited by TDAG8-antagonist (NSC745885) and $Na_v1.8$-blocker (A803467) treatment. In Group IV, acid-induced sodium signals were not inhibited by TDAG8-antagonist (NSC745885) treatment but were inhibited by $Na_v1.8$-blocker (A803467) treatment. Approximately half of <20-μm diameter neurons (46% in IB4+ and 58% in IB4- neurons) were Group I neurons (TDAG8 and $Na_v1.8$ co-expressing neurons). Accordingly, TDAG8 activation may regulate $Na_v1.8$ function in both IB4(+) and IB4(−) neurons in the acute CCI phase.

T cell death-associated gene 8 activation regulates $Na_v1.8$ function via hyperpolarization-activation cyclic nucleotide-gated ion channel in IB4(+) dorsal root ganglia neurons in the early chronic constriction injury phase

TDAG8 activation induced cAMP accumulation and PKA activation. To address whether the TDAG8-cAMP-PKA pathway regulates $Na_v1.8$ function, a PKA inhibitor (H89) was injected into mice at different weeks after CCI. The PKA inhibitor inhibited CCI-induced mechanical allodynia at weeks 3 and 4 (Figure 4A). We then used primary DRG neurons to examine whether acid-induced sodium signaling is mediated by PKA. Treatment with a TDAG8 antagonist (NSC745885) and PKA inhibitor (H89) revealed DRG neurons divided into two groups: Group I neurons showed TDAG8-and PKA-dependent sodium signals and Group II presented TDAG8-independent sodium signals (Figure 4B). It confirmed that the TDAG8-cAMP-PKA pathway is able to regulate acid-induced sodium signals.

Because $Na_v1.8$ participates mainly in the first 2 weeks after CCI (Figure 3E), molecules other than PKA could be more important in regulating $Na_v1.8$ function. Deletion of HCN2, a cAMP-gated calcium channel, in $Na_v1.8$-expressing neurons, abolished CCI-induced mechanical allodynia.[32] TDAG8 activation-increased cAMP may bind directly to and activate HCN2, then regulate $Na_v1.8$ function. To test this hypothesis, we intraplantarly injected an HCN blocker (ZD7288) into mice at week 1 after CCI and found that the peak of ZD7288-induced inhibitory effect at 2–3 h (Figure 4C). The time point of 2 h for ZD7288 was used for further analysis. ZD7288 was then injected into mice at different weeks after CCI. The HCN blocker inhibited CCI-induced mechanical allodynia at 1–2 weeks (Figure 4D).

To further confirm the HCN action by type neurons, we examined calcium signals at week 2 after CCI in ZD7288-injected mice. Acid-induced calcium signals were significantly inhibited by ZD7288 in <20-μm diameter IB4(+) neurons but not <20-μm diameter IB4(−) neurons

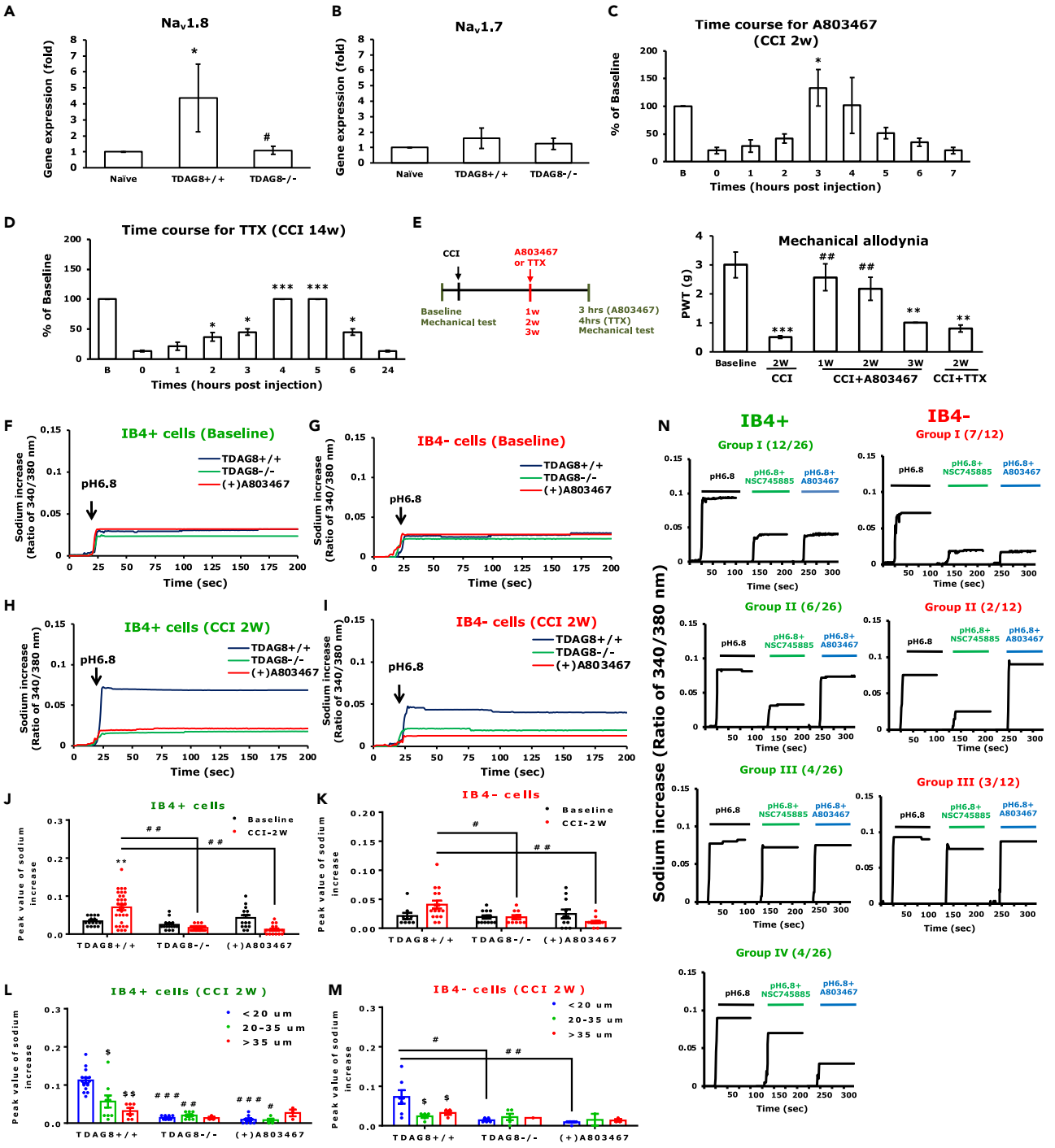

Figure 3. TDAG8-mediated $Na_v1.8$ signaling is involved in the early phase of CCI-induced mechanical allodynia

(A and B) L4-6 DRG from naive, $TDAG8^{+/+}$, or $TDAG8^{-/-}$ mice were taken at 2 weeks after CCI surgery. RT-qPCR analysis of $Na_v1.8$ (A) and $Na_v1.7$ (B) gene expression. $TDAG8^{+/+}$ vs. naive *$p = 0.038$; $TDAG8^{-/-}$ vs. $TDAG8^{+/+}$ #$p = 0.041$ by one-way ANOVA with a post-hoc Bonferroni test. $N = 3$ male and female mice for each group.

(C) The time course of $Na_v1.8$ antagonist A8303467. A8303467 was intraplanarly injected into male mice at 2 weeks after CCI, followed by a mechanical test. PWTs of A8303467-untreated (0 h) or -treated mice (1–7 h) were normalized by PWT of naive mice as a baseline control. *$p = 0.032$ for A8303467-treated vs. untreated group by one-way ANOVA with a post-hoc Bonferroni test. $N = 6$ mice.

Figure 3. *Continued*

(D) The time course of Tetrodotoxin (TTX). TTX was intraplanarly injected into male mice at 14 weeks after CCI, followed by a mechanical test. PWTs of TTX-untreated (0 h) or -treated mice (1–6, 24 h) were normalized by PWT of naive mice as a baseline control. *$p < 0.05$, ***$p < 0.001$ for TTX-treated vs. untreated group. Untreated vs. TTX-2h $p = 0.041$; untreated vs. TTX-3h $p = 0.032$; untreated vs. TTX-4h $p < 0.001$; untreated vs. TTX-5h $p < 0.001$; untreated vs. TTX-6h $p = 0.031$ by one-way ANOVA with a post-hoc Bonferroni test. $N = 6$ mice.

(E) A8303467 was separately intraplanarly injected at 1, 2, and 3 weeks after CCI, then male mice underwent mechanical tests. TTX was intraplanarly injected at 2 weeks after CCI, then male mice underwent mechanical tests. **$p < 0.01$, ***$p < 0.001$, CCI or CCI+ drug vs. baseline; #$p < 0.05$ CCI vs. CCI+ drug. Untreated vs. TTX-2h $p = 0.041$; untreated vs. TTX-3h $p = 0.032$; untreated vs. TTX-4h $p < 0.001$; untreated vs. TTX-5h $p < 0.001$; untreated vs. TTX-6h $p = 0.031$ by one-way ANOVA with a post-hoc Bonferroni test. $N = 6$ mice for each treatment group. Data are mean ± SEM of PWT.

(F–M) Intracellular sodium signals were recorded at baseline or 2 weeks after CCI in TDAG8$^{+/+}$, TDAG8$^{-/-}$, or A803467-injected mice. The time course of sodium signals is shown in F-I and mean ± SEM peak values are presented in J–M. **$p < 0.01$ for baseline vs. 2 weeks; #$p < 0.05$, ##$p < 0.01$, ###$p < 0.001$ for TDAG8$^{+/+}$ vs. TDAG8$^{-/-}$ or A803467 treatment; \$$p < 0.05$, \$\$$p < 0.01$ for <20-μm diameter neurons vs. 20- to 35-μm or >35-μm diameter neurons by one -way ANOVA with a post-hoc Bonferroni test. (J) TDAG8$^{+/+}$ CCI-2w vs. TDAG8$^{+/+}$ baseline $p = 0.003$; TDAG8$^{+/+}$ CCI-2w vs. TDAG8$^{-/-}$ CCI-2w $p = 0.004$; TDAG8$^{+/+}$ CCI-2w vs. A803467 CCI-2w $p = 0.002$. (K) TDAG8$^{+/+}$ CCI-2w vs. TDAG8$^{-/-}$ CCI-2w $p = 0.021$, TDAG8$^{+/+}$ CCI-2w vs. A803467 CCI-2w $p = 0.005$. (L) < 20 μm TDAG8$^{+/+}$ vs. 20–35 μm TDAG8$^{+/+}$ $p = 0.039$; <20 μm TDAG8$^{+/+}$ vs. > 35 μm TDAG8$^{+/+}$ $p = 0.008$; <20 μm TDAG8$^{+/+}$ vs. < 20 μm TDAG8$^{-/-}$p<0.001; in 20–35 μm TDAG8$^{+/+}$ vs. 20–35 μm TDAG8$^{-/-}$ $p = 0.007$; <20 μm TDAG8$^{+/+}$ vs. < 20 μm A803467 $p < 0.001$; 20–35 μm TDAG8$^{+/+}$ vs. 20–35 μm A803467 $p = 0.003$. (M) < 20 μm TDAG8$^{+/+}$ vs. 20–35 μm TDAG8$^{+/+}$ $p = 0.041$; >35 μm TDAG8$^{+/+}$ vs. > 35 μm TDAG8$^{+/+}$ $p = 0.043$; <20 μm TDAG8$^{+/+}$ vs. <20 μm TDAG8$^{-/-}$p = 0.012; <20 μm TDAG8$^{+/+}$ vs. < 20 μm A803467 $p = 0.002$.

(N) DRG neurons from naive male mice were sequentially stimulated with pH 6.8, pH 6.8+TDAG8 antagonist (NSC745885), and pH 6.8 + A8303467, and sodium signals were recorded, followed by IB4 staining. The time course of sodium signals is shown in N. Significant symbols used in figures are defined as such: *$p < 0.05$, **$p < 0.01$, ***$p < 0.001$, #$p < 0.05$; ##$p < 0.01$, ###$p < 0.001$, \$$p < 0.05$, \$\$$p < 0.01$.

(Figures 4E and 4F). Treatment with a TDAG8 antagonist (NSC745885) and HCN inhibitor (ZD7288) revealed DRG neurons divided into three groups: Group I neurons showed TDAG8-and HCN-dependent calcium signals; Group II only had TDAG8-dependent calcium signals; and Group III no TDAG8-and HCN-dependent calcium signals (Figures 4G and 4H). Many naive IB4(+) neurons (66%) showed TDAG8-and HCN-dependent calcium signals, but only 20% of IB4(−) neurons showed TDAG8-and HCN-dependent calcium signals (Figures 4G and 4H). TDAG8-meidated calcium signals may be regulated by HCN in IB4(+) neurons and other molecules in IB4(−) neurons.

We examined acid-induced sodium signals at 2 weeks after CCI. Acid-induced sodium signals were inhibited by HCN blocker treatment in <20-μm diameter IB4(+) but not IB4(−) neurons (Figures 4I and 4J). Three groups of sodium signal patterns were found: Group I was HCN- and Nav1.8-dependent, Group II was Nav1.8-dependent, and Group III was HCN- and $Na_v1.8$-independent (Figures 4K and 4L). In more than half (63%) of IB4(+) neurons, sodium signals were inhibited by HCN and $Na_v1.8$ blocker treatment (Figures 4K and 4L). Accordingly, TDAG8 activation may modulate $Na_v1.8$ function via HCN mainly in IB4(+) neurons.

To confirm whether IB4(+) neurons are involved in the early phase of mechanical allodynia, we intrathecally administered IB4-saporin (IB4-Sap) to mice before (−1 week) CCI surgery to deplete IB4(+) neurons. According to the previous study,[33] the intrathecal injection of IB4-Sap in mice depletes non-peptidergic C fiber population, decreasing P2X3 and TRPV1 expression in DRG and IB4(+) labeling in the spinal cord. Ablation of IB4(+) neurons before CCI inhibited CCI-induced mechanical allodynia for at least 3 weeks (Figure 5A). We then examined the acid-responding cell proportion and calcium signals in mice injected with SAP/IB4-SAP before CCI. Acid-induced calcium signals at week 2 were reduced in frequency after IB4-sap treatment in IB4(+) neurons, with no change in IB4(−) neurons (Figures 5B–5D). At week 14, acid-induced calcium signals were unchanged in frequency (Figures 5E and 5F). The proportion of responsive IB4(+) neurons was reduced from 48% to 20% at 2 weeks after CCI surgery, with no reduction found at 14 weeks (Figure 5G). Removal IB4(+) neurons before CCI surgery may reduce acid-responsive IB4(+) neurons and acid-induced calcium signal frequency and delay the development of mechanical allodynia.

Accordingly, TDAG8 activation increased cAMP accumulation to activate HCN, which modulated $Na_v1.8$ function to initiate mechanical allodynia in IB4(+) neurons. TDAG8 activation could also regulate $Na_v1.8$ function in IB4(−) neurons via other molecules, thus enhancing pain hypersensitivity.

T cell death-associated gene 8 deficiency reduces local inflammation by decreasing M1/M2 macrophage ratio

IB4(+) neurons are the major neurons for the initiation of mechanical allodynia, IB4(−) neurons could also have some role in facilitating the development of mechanical allodynia. TDAG8 activation could also regulate $Na_v1.8$ function in IB4(−) neurons via other molecules, controlling SP release to modulate local inflammation. To address this question, we first examined whether nerve injury-caused long-term local inflammation is regulated by TDAG8 activation.

As expected, TDAG8$^{+/+}$ mice exhibited long-term inflammation after CCI (Figure 6A). The number of total immune cells was increased over time (Figure 6B): the granulocyte number was increased in the first week (Figure 6C), the macrophage number was increased over time (Figure 6D), and the lymphocyte number was unchanged as compared with 0 weeks (before CCI surgery) (Figure 6E). In TDAG8-deficient mice, although the number of total immune cells also increased over time, the number was greatly reduced at weeks 1 and 2 (the early phase) and 8 and 14 (the late phase) as compared with TDAG8$^{+/+}$ mice (Figures 6A and 6B). The granulocyte number was decreased at week 1 (Figure 6C), and macrophage numbers were reduced at weeks 2, 8, and 14 as compared with TDAG8$^{+/+}$ mice (Figure 6D). Such a decrease was associated with attenuated mechanical allodynia in TDAG8$^{-/-}$ mice.

Two different macrophage phenotypes, M1 (classically activated) and M2 (alternatively activated), are responsible for producing pro-inflammatory and anti-inflammatory cytokines, respectively.[34] To further understand which macrophage type was the major contributor to

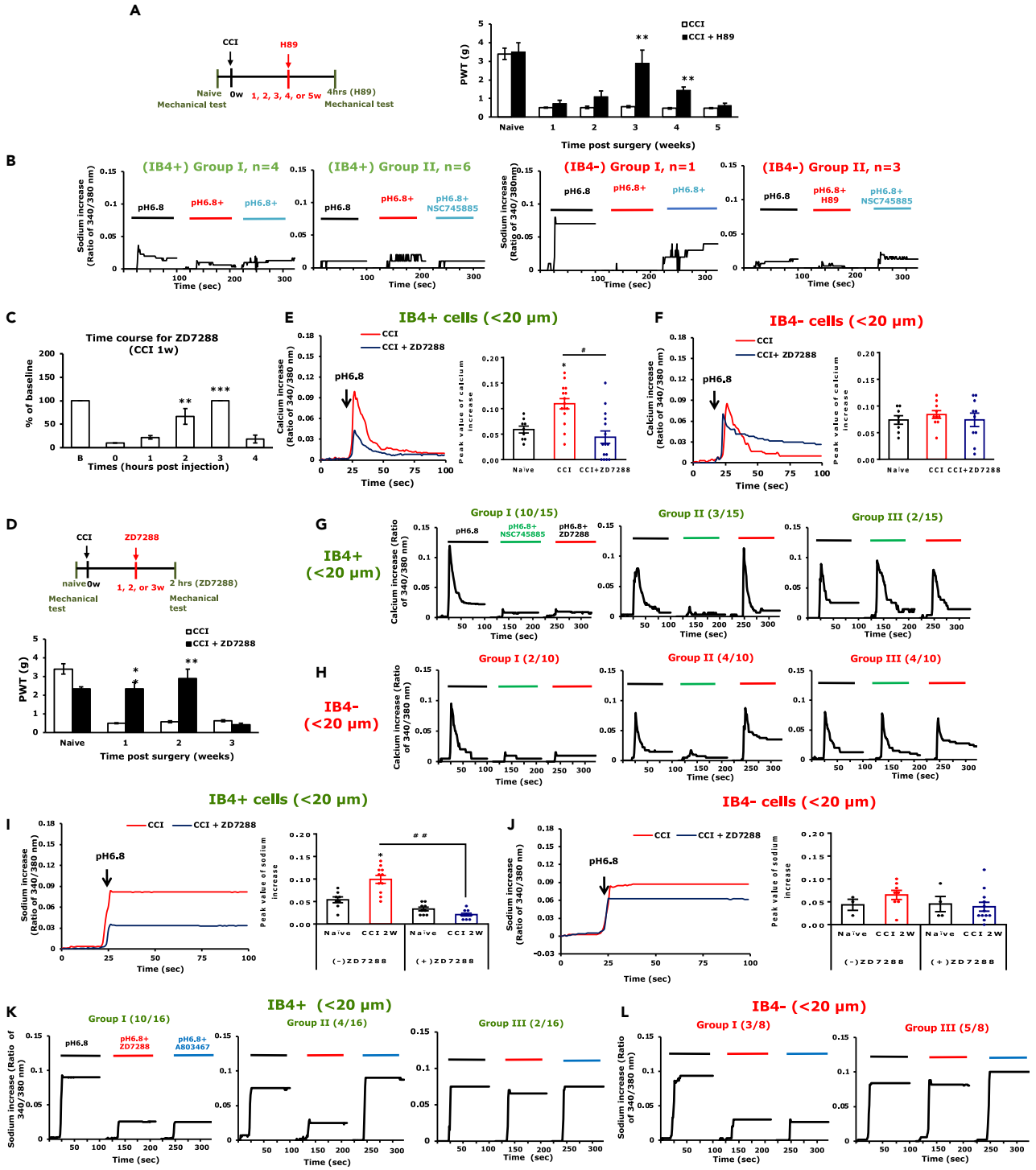

Figure 4. HCN signaling is involved in the early phase of CCI-induced mechanical allodynia in IB4(+) neurons

(A) PKA inhibitor H89 was intraplanarly injected at 1, 2, 3, 4, and 5 weeks after CCI, then male mice underwent mechanical tests. CCI+H89 vs. CCI-2w $^{**}p = 0.006$; CCI+H89 vs. CCI-4w $^{*}p = 0.021$ by two-way ANOVA with a post-hoc Bonferroni test. $N = 6$ mice for each treatment group. Data are mean ± SEM of PWT.

(B) DRG neurons from TDAG8$^{+/+}$ female mice were sequentially stimulated with pH 6.8, pH 6.8 + H89 (PKA inhibitor), and pH 6.8+ NSC745885 (TDAG8 blocker), and sodium signals were recorded, followed by IB4 staining. The time course of sodium signals in IB4(+) neurons is shown in the upper panels and in $IB_4(-)$ neurons in the lower panels.

Figure 4. *Continued*

(C) The time course of HCN blocker ZD7288. ZD7288 was intraplanarly injected into male mice at 1 week after CCI, followed by a mechanical test. PWTs of ZD7288-untreated (0 h) or -treated mice (1–4 h) were normalized by PWT of naive mice as a baseline control. ZD7288-2h vs. 0h $^{**}p = 0.008$; ZD7288-3h vs. 0h $^{***}p < 0.001$ by one-way ANOVA with a post-hoc Bonferroni test. $N = 6$ mice.

(D) ZD7288 was intraplanarly injected at 1, 2, and 3 weeks after CCI, then male mice underwent mechanical tests. CCI vs. CCI+ZD7288-1w $p = 0.002$; CCI vs. CCI+ZD7288-2w $p = 0.003$ by two-way ANOVA with a post-hoc Bonferroni test. $N = 6$ mice for each treatment group. Data are mean ± SEM.

(E and F) Intracellular calcium signals were recorded at 2 weeks after CCI in naive, CCI, or CCI+ZD7288 mice, followed by IB4 staining. Presents time course of calcium signals and mean ± SEM peak values. $^{*}p < 0.05$ for naive vs. CCI or CCI+ZD7288 mice; $\#p < 0.05$ for CCI vs. CCI+ZD7288 mice. Naive vs. CCI $p = 0.031$; CCI vs. CCI+ZD7288 $p = 0.039$ by one-way ANOVA with a post-hoc Bonferroni test.

(G and H) DRG neurons from naive mice were sequentially stimulated with pH 6.8, pH 6.8+TDAG8 antagonist (NSC745885), and pH 6.8+ ZD7288, and calcium signals were recorded, followed by IB4 staining. The time course of calcium signals in IB4(+) neurons is shown in F and in IB4(−) neurons in G.

(I and J) Intracellular sodium signals were recorded at 2 weeks after CCI in naive or ZD7288-treated mice, followed by IB4 staining. The time course of sodium signals and mean ± SEM peak values are presented. $^{*}p = 0.029$ for naive vs. CCI+ZD7288 mice; CCI vs. CCI+ZD7288 $\#\#p = 0.005$ by one-way ANOVA with a post-hoc Bonferroni test.

(K and L) DRG neurons from naive mice were sequentially stimulated with pH 6.8, pH 6.8+ZD7288 (HCN blocker), and pH 6.8 + A803467 ($Na_v1.8$ blocker), and sodium signals were recorded, followed by IB4 staining. The time course of sodium signals in IB4(+) neurons is shown in K and in IB_4(−) neurons in L. PWT, paw withdrawal threshold.

mechanical allodynia, we used anti-CD80 and anti-CD163 antibodies to distinguish M1 and M2 macrophages, respectively. $TDAG8^{+/+}$ CCI mice showed a higher $CD80^{+}$ than CD163+ number, and the ratio of M1/M2 macrophages remained high from weeks 1–14 (M1/M2 = 80/20) (Figures 6F–6I), In $TDAG8^{-/-}$ CCI mice, the $CD80^{+}$ macrophage number was decreased at weeks 2, 8, and 14, but the CD163+ macrophage number was increased at weeks 1, 8 and 14 (Figures 6F–6H). The ratio of M1/M2 macrophages in $TDAG8^{-/-}$ mice was decreased from week 1 as compared with $TDAG8^{+/+}$ mice (M1/M2 = 40/60 at 1 week for $TDAG8^{-/-}$; M1/M2 = 80/20 at 1 week for $TDAG8^{+/+}$) (Figures 6I and 6J). Pro-inflammatory cytokines, TNFα, IL-6, and anti-inflammatory cytokine IL-10 were also examined in injured sciatic nerve (Figures 6K–6M). In $TDAG8^{+/+}$ mice TNFα and IL-6 levels were increased at 2, 14w after CCI, but IL-10 was kept at a low level. TDAG8 deletion reduced IL-6 level and increased IL-10 level at 2, 14w but did not change TNFα level. We also examined macrophage number and cytokine levels in DRG. As shown in Figure 7, M1 macrophage number was increased in DRG at 2, 14 w after CCI in $TDAG8^{+/+}$ mice and TDAG8 deletion decreased M1 macrophage number (Figure 7A). M2 macrophage number remained unchanged in both $TDAG8^{+/+}$ and $TDAG8^{-/-}$ mice (Figure 7B). TNFα level was increased at 2w after CCI in $TDAG8^{+/+}$ mice and such level was reversed by TDAG8 deletion (Figure 7C). IL-6 level was increased at 14w after CCI in $TDAG8^{+/+}$ mice but not reversed in $TDAG8^{-/-}$ mice (Figure 7D). IL-10 level was unchanged in both mice (Figure 7E).

To further confirm the macrophage could be critical to attenuating the early phase of mechanical allodynia, a macrophage inhibitor clodronate (CLD) was injected into mice at weeks 1–4 after CCI surgery. CLD (1 mg) partially attenuates CCI-induced mechanical allodynia in the early phase (Figure 7F). Administration of CLD greatly inhibited an increase in the M1 macrophage number but did not change the M2 macrophage number as compared with vehicle controls (Figure 7G). The ratio of M1/M2 macrophages decreased after CLD injection (M1/M2 ratio 70/30 in vehicle control and 50/50 with CLD injection) (Figure 7H). Thus, TDAG8 activation modulated the M1/M2 macrophage ratio to regulate the early phase of mechanical allodynia.

T cell death-associated gene 8-dependent substance P release in the periphery enhances IB4(+) neuron activity by regulating M1/M2 macrophage balance and $Na_v1.8$ level in the early phase

Given that TDAG8 activation modulates IB4(−) neuron activity (Figure 2), TDAG8 activation likely regulates SP release from IB4(−) neurons directly to transduce signals to the spinal cord or indirectly to modulate local inflammation, further enhancing pain hypersensitivity. To examine whether SP release at the sciatic nerve regulates local inflammation and pain, we locally delivered the NK_1 receptor agonist Sar-Met-SP around the sciatic nerve 1 week after CCI surgery in mice. With Sar-Met-SP administration at 1 week in $TDAG8^{-/-}$ CCI mice, TDAG8 deficiency-dependent attenuation was reversed in the early phase (2, 3 weeks) but not late phase of mechanical allodynia (Figure 8A).

We then examined whether SP regulates macrophages to enhance local inflammation. TDAG8 deletion reduced M1 number at both weeks 2 and 14. As expected, Sar-Met-SP administration reversed the reduced number of M1 macrophages at week 2 but not at week 14 (Figures 8B–8E). M2 macrophage number was increased at week 14 but not at week 2 in TDAG8-deficient mice and Sar-Met-SP–administered mice (Figures 8B, 8D, and 8F). Hence, Sar-Met-SP administration reversing the anti-nociceptive effect of TDAG8 deletion in the early phase could be due in part to reduced M1 macrophage number. TDAG8 regulated SP release in the periphery to recruit M1 macrophages to the injured sciatic nerve, thus facilitating the early phase of mechanical allodynia.

To understand whether SP action on local inflammation is due to the modulation of neuron activity, we examined calcium signals in $TDAG8^{+/+}$, $TDAG8^{-/-}$, and Sar-Met-SP/$TDAG8^{-/-}$ DRG cultures after challenge with pH 6.8. CCI-increased calcium signals were inhibited by TDAG8 deletion in IB4(+) DRG neurons at week 2, but such inhibition was reversed after the addition of Sar-Met-SP (Figures 8G and 8H). IB4(−) neurons showed no significant changes in calcium signals (Figures 8I and 8J). Of note, the reversal of calcium signals mainly occurred in <20-μm diameter IB4(+) neurons (Figure 8K) but not IB4(−) neurons (Figure 8L), which agreed with IB4(+) neurons being the major contributor to the early mechanical allodynia (Figure 5). Given that $Na_v1.8$ mediates the early phase of mechanical allodynia (Figure 3C), we also examined $Na_v1.8$ gene expression. $Na_v1.8$ expression suppressed by TDAG8 deletion was reversed by local Sar-Met-SP delivery

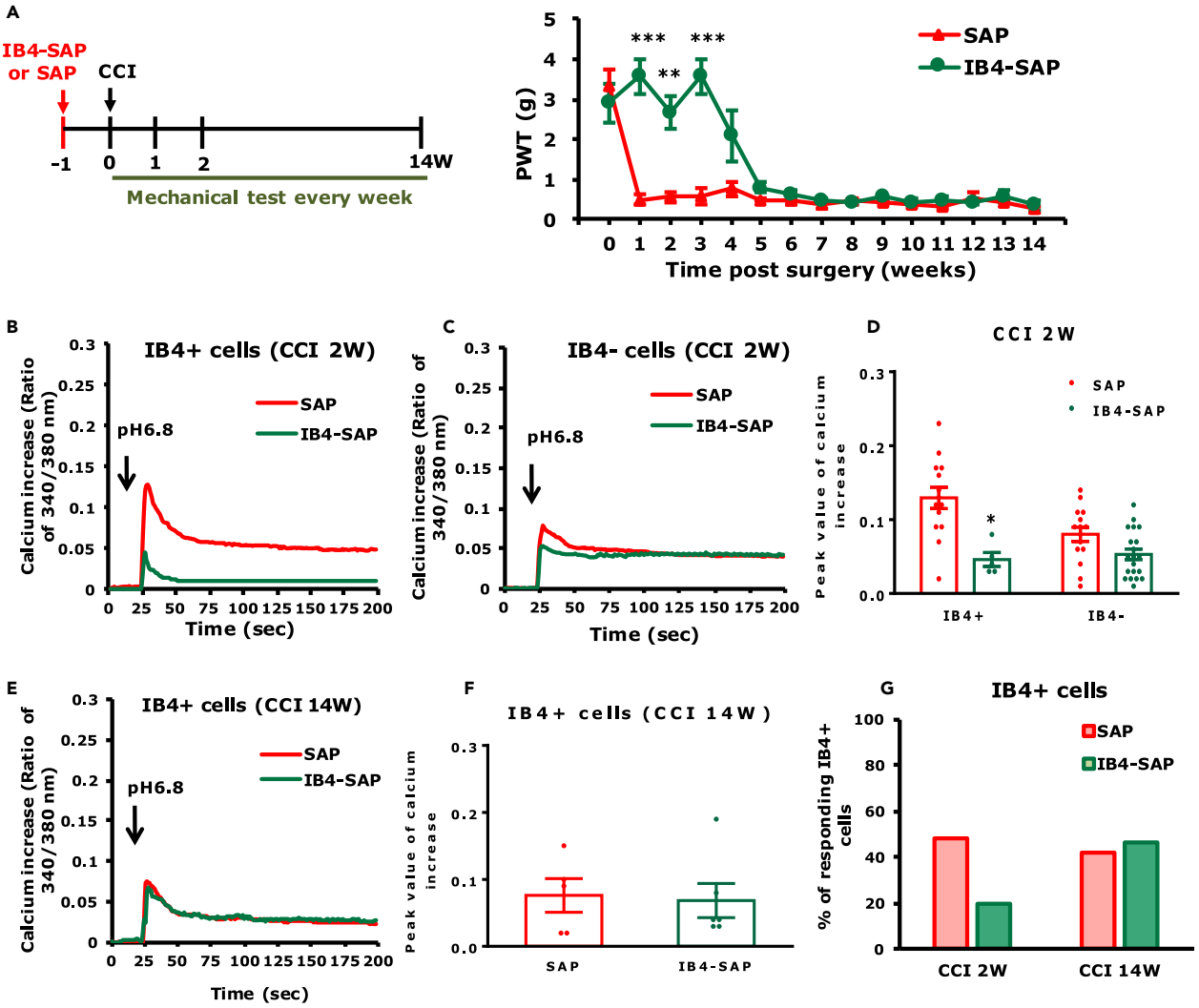

Figure 5. IB_4(+) neurons are involved in the early phase of CCI-induced mechanical allodynia

(A–C) IB4-saporin (IB4-SAP) or saporin (SAP) was intrathecally injected into male mice at 1 week before (−1 week) CCI surgery, followed by mechanical tests (A). $^{**}p < 0.01$, $^{***}p < 0.001$ for SAP vs. IB4-SAP. IB4-SAP-1w vs. SAP-1w $^{***}p < 0.001$; IB4-SAP-2w vs. SAP-2w $^{**}p < 0.007$, IB4-SAP-3w vs. SAP-3w $^{***}p < 0.001$ by two-way ANOVA with a post-hoc Bonferroni test. (B–G) L4-6 DRG from IB4-SAP or SAP-injected male and female mice were taken at 2 or 14 weeks after CCI, followed by calcium imaging. Time course of calcium signals at 2 weeks after CCI in (B) IB4(+) neurons and (C) IB4(−) neurons.

(D) Mean ± SEM peak values of calcium signals at 2 weeks. IB4-SAP vs. SAP $p = 0.038$ in IB4(+) neurons by one-way ANOVA with a post-hoc Bonferroni test.

(E) Time course of calcium signals at 14 weeks after CCI in IB4(+) neurons.

(F) Mean ± SEM peak values of calcium signals at 14 weeks.

(G) The percentage of responding neurons. Significant symbols used in figures are defined as such: $^{*}p < 0.05$, $^{**}p < 0.01$, $^{***}p < 0.001$.

(Figure 8M). $Na_v1.7$ gene expression was not changed (Figure 8N). These results suggest that TDAG8 may regulate SP release peripherally to recruit M1 macrophages, increase $Na_v1.8$ gene expression, and increase calcium signals in IB4(+) neurons to enhance pain hypersensitivity.

T cell death-associated gene 8-dependent substance P release in soma and regulation of satellite glial cell number and $Na_v1.7$ expression in the late phase of mechanical allodynia

Administration of NK_1 agonist Sar-Met-SP could reverse the anti-nociceptive effect of TDAG8 deletion in the early but not late phase of mechanical allodynia (Figure 8A), which suggests that peripheral SP release has a more substantial effect on the early than late phase. To understand whether SP action is critical to the late phase of mechanical allodynia, we intrathecally injected RP67580 (NK1 receptor antagonist) into mice at 1 week after CCI surgery. TDAG8 deficiency-dependent recovery of the chronic mechanical allodynia (14–17 weeks) was reversed after RP67580 administration at week 1 in $TDAG8^{-/-}$ mice (Figure 9A), which suggests that SP release in DRG in the early phase (1 week) may have an anti-nociceptive role. We then examined $Na_v1.7$ and 1.8 channel gene expression at 14 weeks in $TDAG8^{+/+}$, $TDAG8^{-/-}$, and

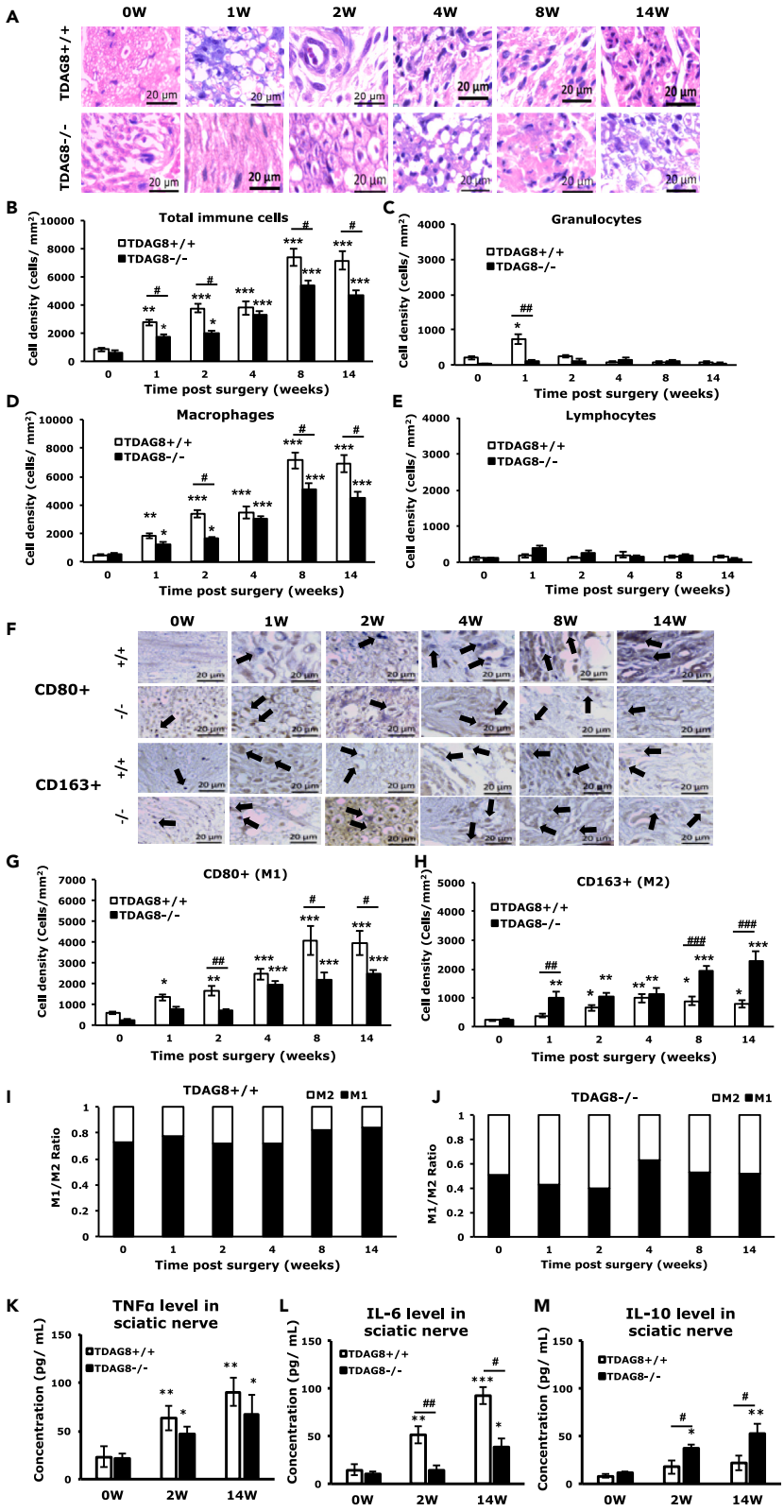
A
0W
1W
2W
4W
8W
14W
TDAG8+/+
TDAG8-/-
20 μm
B
Total immune cells
Cell density (cells/ mm²)
TDAG8+/+
TDAG8-/-
Time post surgery (weeks)
C
Granulocytes
D
Macrophages
E
Lymphocytes
F
CD80+
CD163+
+/+
-/-
G
CD80+ (M1)
Cell density (Cells/mm²)
H
CD163+ (M2)
I
TDAG8+/+
M2 M1
M1/M2 Ratio
J
TDAG8-/-
K
TNFα level in sciatic nerve
Concentration (pg/ mL)
L
IL-6 level in sciatic nerve
M
IL-10 level in sciatic nerve

Figure 6. Deletion of TDAG8 decreases the ratio of M1/M2 macrophages after CCI

The sciatic nerves of TDAG8$^{+/+}$ or TDAG8$^{-/-}$ male mice were taken at 0, 1, 2, 4, 8, and 14 weeks after CCI surgery, fixed and sectioned, then underwent H&E staining.

(A) Representative nerve images of different types of immune cells. Scale bar = 20 μm.

(B–E) Cell density of total immune cells (B), granulocytes (C), macrophages (D), and lymphocytes (E) was obtained by calculating the total cell number from a 1-mm^2 region. Data are mean ± SEM. (B) 0w vs. 1w $p = 0.005$, 0w vs. 2, 4, 8 and 14w $p < 0.001$ in TDAG8$^{+/+}$ mice; 0w vs. 1w $p = 0.034$, 0w vs. 2w $p = 0.031$, 0w vs. 4, 8 and 14w $p < 0.001$ in TDAG8$^{-/-}$ mice; TDAG8$^{-/-}$ vs. TDAG8$^{+/+}$ at 1w $p = 0.043$; 2w $p = 0.038$; 8w $p = 0.039$; 14w $p = 0.020$. (C) 0w vs. 1w $p = 0.031$ in TDAG8$^{+/+}$ mice; TDAG8$^{-/-}$ vs. TDAG8$^{+/+}$ at 1w $p = 0.004$. (D) 0w vs. 1w $p = 0.002$, 0w vs. 2, 4, 8 and 14w $p < 0.001$ in TDAG8$^{+/+}$ mice; 0w vs. 1w $p = 0.043$, 0w vs. 2w $p = 0.039$, 0w vs. 4, 8 and 14w $p < 0.001$ in TDAG8$^{-/-}$ mice; TDAG8$^{-/-}$ vs. TDAG8$^{+/+}$ at 2w $p = 0.039$; 8w $p = 0.023$; 14w $p = 0.020$. *$p < 0.05$, **$p < 0.01$, ***$p < 0.001$ for 0 weeks vs. other weeks; #$p < 0.05$; ##$p < 0.01$ for TDAG8$^{-/-}$ vs. TDAG8$^{+/+}$ by two-way ANOVA with a post-hoc Bonferroni test.

(F–J) Sections were stained with anti-CD80 or anti-CD163 antibodies. Cell images are presented in F and arrows indicate macrophages. Cell density of CD80$^+$ (G) or CD163$^+$ (H) macrophages was obtained by calculating the total cell number from a 1-mm^2 region. (G) 0w vs. 1w $p = 0.021$, 0w vs. 2w $p = 0.009$, 0w vs. 4, 8 and 14w $p < 0.001$ in TDAG8$^{+/+}$ mice; 0w vs. 4, 8 and 14w $p < 0.001$ in TDAG8$^{-/-}$ mice; TDAG8$^{-/-}$ vs. TDAG8$^{+/+}$ at 2w $p = 0.007$, 8w $p = 0.041$, 14w $p = 0.039$. (H) 0w vs. 2w $p = 0.032$, 0w vs. 4w $p = 0.009$, 0w vs. 8w $p = 0.012$, 0w vs. 14w $p = 0.019$ in TDAG8$^{+/+}$ mice; 0w vs. 1w $p = 0.007$, 0w vs. 2w $p = 0.006$; 0w vs. 4w $p = 0.007$; 0w vs. 8w $p < 0.001$; 0w vs. 14w $p < 0.001$ in TDAG8$^{-/-}$ mice; TDAG8$^{-/-}$ vs. TDAG8$^{+/+}$ at 1w $p = 0.005$, at 8w and 14w $p < 0.001$. *$p < 0.05$, **$p < 0.01$, ***$p < 0.001$ for 0 weeks vs. other weeks; #$p < 0.05$; ##$p < 0.01$; ###$p < 0.001$ for TDAG8$^{+/+}$ vs. TDAG8$^{-/-}$ by two-way ANOVA with a post-hoc Bonferroni test. Ratio of M1 and M2 macrophages in TDAG8$^{+/+}$ (I) and TDAG8$^{-/-}$ (J) in sciatic nerves. $N = 3$ mice for each group. Data are mean ± SEM.

(K–M) Sciatic nerves from TDAG8$^{+/+}$ and TDAG8$^{-/-}$ male mice were taken at 0, 2, and 14w after CCI and homogenized, followed by analysis of TNFα (K), IL-6 (L), and IL-10 (M) using ELISA kits. Data are mean ± SEM. $N = 3$ mice. (K) 0w vs. 2w $p = 0.007$, 0w vs. 14w $p = 0.006$ in TDAG8$^{+/+}$ mice; 0w vs. 2w $p = 0.018$, 0w vs. 14w $p = 0.034$ in TDAG8$^{-/-}$ mice. (L) 0w vs. 2w $p = 0.005$, 0w vs. 14w $p < 0.001$ in TDAG8$^{+/+}$ mice; 0w vs. 14w $p = 0.031$ in TDAG8$^{-/-}$ mice; TDAG8$^{-/-}$ vs. TDAG8$^{+/+}$ at 2w $p = 0.007$, 8w $p = 0.019$, 14w $p = 0.019$. (M) 0w vs. 2w $p = 0.028$, 0w vs. 14w $p = 0.006$ in TDAG8$^{-/-}$ mice; TDAG8$^{-/-}$ vs. TDAG8$^{+/+}$ at 2w $p = 0.041$, 14w $p = 0.032$. Significant symbols used in figures are defined as such: *$p < 0.05$, **$p < 0.01$, ***$p < 0.001$, #$p < 0.05$, ##$p < 0.01$, ###$p < 0.001$.

RP67580/TDAG8$^{-/-}$ DRG. The expression of Na$_v$1.7 but not Na$_v$1.8 gene was significantly increased at 14 weeks and was inhibited by TDAG8 deletion (Figures 9B and 9C). RP67580 intrathecal administration in TDAG8$^{-/-}$ mice reversed the downregulation of Na$_v$1.7 expression, with no change from the control in TDAG8 and Na$_v$1.8 gene expression (Figures 9B and 9C). We then injected the TTX into CCI mice at week 14 and found mechanical allodynia attenuated at week 14 (Figure 9D). Given that Na$_v$1.7 gene expression was upregulated at week 14, Na$_v$1.7 may be the major channel involved in the late phase of mechanical allodynia. SP release in soma inhibited Na$_v$1.7 gene expression, thereby attenuating the late phase of mechanical allodynia.

To understand whether RP67580 action is due to the modulation of sodium channels, we examined sodium signals in TDAG8$^{+/+}$, TDAG8$^{-/-}$, and RP67580/TDAG8$^{-/-}$ DRG cultures after challenge with pH 6.8. IB4(+) neurons showed no significant changes in sodium signals (Figure 9E). CCI-increased sodium signals were inhibited by TDAG8 deletion in IB4(−) DRG neurons at week 14, but such inhibition was reversed after the addition of RP67580 (Figure 9F), which agreed with the Na$_v$1.7 expression change. Of note, reversal of sodium signals mainly occurred in 20- to 35-μm and >35-μm diameter IB4(−) neurons, but not IB4(+) neurons (Figures 9G and 9H), which agreed with IB4(−) neurons being the major contributor to the late mechanical allodynia (Figure 2).

SGCs modulate the neuron activities for the development of chronic hyperalgesia. SP release from DRG neurons may control SGC activation. Thus, we also examined whether TDAG8 deletion reduced SGC number. The number of SGCs in TDAG8$^{+/+}$ DRG was greatly increased from the first week after CCI, peaked at week 2, and was maintained for up to 14 weeks (Figures 9I and 9J). In TDAG8$^{-/-}$ mice, the number of SGCs increased at week 1, but a low number of SGCs was maintained for 14 weeks (Figures 9I and 9J). The number of SGCs was lower in TDAG8$^{-/-}$ than in TDAG8$^{+/+}$ DRG. RP67580 administration in TDAG8$^{-/-}$ mice at week 1 reversed the decreased SGC number at weeks 2 and 14 (Figure 9K), which suggests that SP reduced the increase in SGC number. To examine the involvement of SGCs in mechanical allodynia, we intrathecally administrated an SGC inhibitor, fluorocitric acid (FC), at week 2. FC administration blocked the mechanical allodynia from weeks 14–19 (Figure 9L) and reduced the SGC number at weeks 2 and 19 (Figure 9M), which suggests that SGCs may contribute to the chronic phase of mechanical allodynia.

DISCUSSION

In this study, we demonstrated that TDAG8 activation modulated CCI-induced mechanical allodynia by regulating IB4(+) and IB4(−) neuron activity and SP action (Figure 10). TDAG8 activation regulated the HCN and Na$_v$1.8 channels in small IB4(+) neurons, thus initiating mechanical allodynia. TDAG8-cAMP signaling activates PKA and Na$_v$1.8 in small IB4(−) neurons modulated SP release in the periphery, which enhances peripheral inflammation, thereby promoting early mechanical allodynia. Later, SP release in DRG reduced SGC number and Na$_v$1.7 expression, further decreasing neuron activity and preventing the development of late mechanical allodynia. TDAG8 activation increased the activity of medium-to large IB4(−) neurons to overcome the SP-induced inhibitory effect, thus facilitating the late phase of mechanical allodynia.

TDAG8-Na$_v$1.8 signaling in small-diameter IB4(+) neurons initiated injury-induced mechanical allodynia, and TDAG8-cAMP-PKA signaling in small-diameter IB4(−) neurons released SP to induce neurogenic inflammation, thus facilitating the development of early mechanical allodynia. TDAG8-mediated signaling in medium-to large-diameter IB4(−) neurons increased Na$_v$1.7 expression and SGC number to promote late mechanical allodynia, and SP anti-nociceptive effects in soma prevented the development of the late phase.

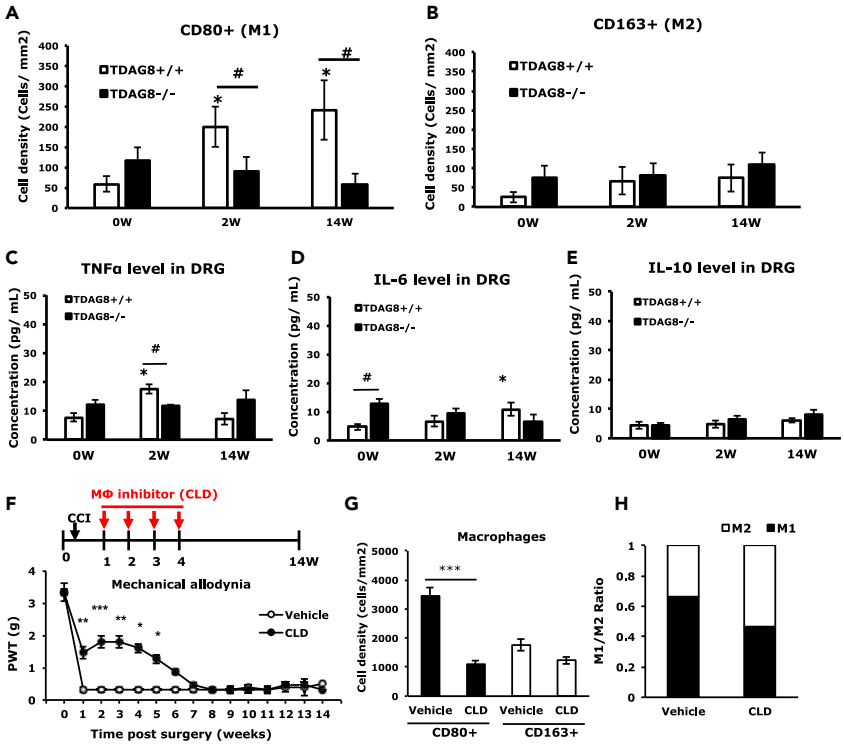

Figure 7. Inhibition of M1 macrophages decreases the ratio of M1/M2 macrophages after CCI

(A and B) L5 DRG of TDAG8$^{+/+}$ or TDAG8$^{-/-}$ male mice were taken at 0, 2, and 14 weeks after CCI surgery, fixed and sectioned, then underwent the staining with anti-CD80 or anti-CD163 antibodies. The cell density of CD80^{+} (A) or CD163^{+} (B) macrophages was obtained by calculating the total cell number from a 1-mm^2 region. (A) TDAG8$^{+/+}$0w vs. TDAG8$^{+/+}$2w $p = 0.033$; TDAG8$^{+/+}$0w vs. TDAG8$^{+/+}$14w $p = 0.043$; TDAG8$^{+/+}$ 2w vs. TDAG8$^{-/-}$ 2w $p = 0.046$, TDAG8$^{+/+}$ 14w vs. TDAG8$^{-/-}$ 14w $p = 0.039$. *$p < 0.05$, for 0 weeks vs. 2 or 14 weeks; #$p < 0.05$ for TDAG8$^{+/+}$ vs. TDAG8$^{-/-}$ by two-way ANOVA with a post-hoc Bonferroni test. $N = 3$ mice for each group. Data are mean ± SEM.

(C–E) L4-6 DRG of TDAG8$^{+/+}$ or TDAG8$^{-/-}$ male mice were taken at 0, 2, and 14 weeks after CCI surgery, followed by the measurement of TNFα (C), IL-6 (D), and IL-10 (E). Data are mean ± SEM. $N = 3$ mice. (C) TDAG8$^{+/+}$0w vs. TDAG8$^{+/+}$ 2w $p = 0.029$; TDAG8$^{+/+}$ 2w vs. TDAG8$^{-/-}$ 2w $p = 0.041$; (D) TDAG8$^{+/+}$ 0w vs. TDAG8$^{+/+}$ 14w $p = 0.041$; TDAG8$^{+/+}$ 0w vs. TDAG8$^{-/-}$ 0w $p = 0.031$. *$p < 0.05$ for 0 weeks vs. 2 or 14 weeks; #$p < 0.05$ for TDAG8$^{+/+}$ vs. TDAG8$^{-/-}$ by two-way ANOVA with a post-hoc Bonferroni test.

(F–H) Clodronate (CLD, 1 mg) or vehicle (veh) was intraperitoneally injected at 1, 2, 3, and 4 weeks after CCI surgery. Paw withdrawal threshold (PWT) (F) was measured before (0 weeks) or 1–14 weeks after surgery. Data are mean ± SEM of PWT ($n = 6$ male mice for each group). CLD vs. vehicle at 1w **$p = 0.008$; 2w ***$p < 0.001$; 3w **$p = 0.007$; 4w *$p = 0.039$; 5w *$p = 0.043$ by two-way ANOVA with post-hoc Bonferroni test. (G) The sciatic nerve from the ipsilateral side of CLD vs. vehicle-injected mice was excised at 4 weeks and the ligature was removed, cross-sectioned, and immunostained with anti-CD80 or anti-CD163 antibody. Scale bar = 20 μm. Cell density of CD80^{+} or CD163^{+} macrophages was obtained by calculating the total cell number from a 1-mm^2 region. ***$p < 0.001$ for CLD vs. vehicle by one-way ANOVA with a post-hoc Bonferroni test. (H) Ratio of M1 and M2 macrophages at 4 weeks in sciatic nerves.

T cell death-associated gene 8 initiates and facilitate the early mechanical allodynia by coordinating IB4(+) and IB4(−) neuron activity

Distinct electrophysiological properties of IB4(+) and IB4(−) neurons determine their functional differences, contributing to the nature of chronic pain.[35,36] IB4(+) neurons have a high density of TTX-resistant (TTX-R) Na^{+} currents.[35,37] TTX-R Na^{+} currents in IB4(+) neurons[35] are similar to the current properties reported for the Na$_v$1.8 channel.[37] Na$_v$1.8 is mainly expressed in IB4(+) neurons.[38] Similar to previous findings,[33,39] ablation of IB4(+) neurons completely abolished the early phase (1–3 weeks) but not the late phase of mechanical allodynia induced by nerve injury (Figure 5A). Pharmacological blockage of Na$_v$1.8 inhibited mechanical allodynia in the first 2 weeks after CCI (Figure 3E), consistent with previous studies.[40–43] Blocking of Na$_v$1.8 also inhibited sodium signals in IB4(+) neurons (Figures 3H, 3J, and 3L). Given that the Na$_v$1.8 channel contributes to the rising phase of the action potential,[44] these findings suggest that the Na$_v$1.8 channel in IB4(+) neurons could be the major receptor responsible for early mechanical allodynia induced by CCI.

TDAG8 deletion attenuated the early phase of mechanical allodynia and inhibited calcium and sodium signals in IB4(+) neurons as well as Na$_v$1.8 gene expression in the first 2 weeks (Figures 1D, 2E, 3A, and 3J). Accordingly, the TDAG8-mediated initiation of mechanical allodynia is likely via the regulation of Na$_v$1.8 in IB4(+) neurons. Because intracellular cAMP level was increased after CCI and blocked by TDAG8 deletion, TDAG8 may regulate Na$_v$1.8 function via cAMP signaling. Deletion of HCN2 in a Na$_v$1.8-expressing mouse population abolished CCI-induced mechanical allodynia and thermal hyperalgesia in the first 3 weeks.[45] Using a non-selective blocker of HCN, we demonstrated that HCN is

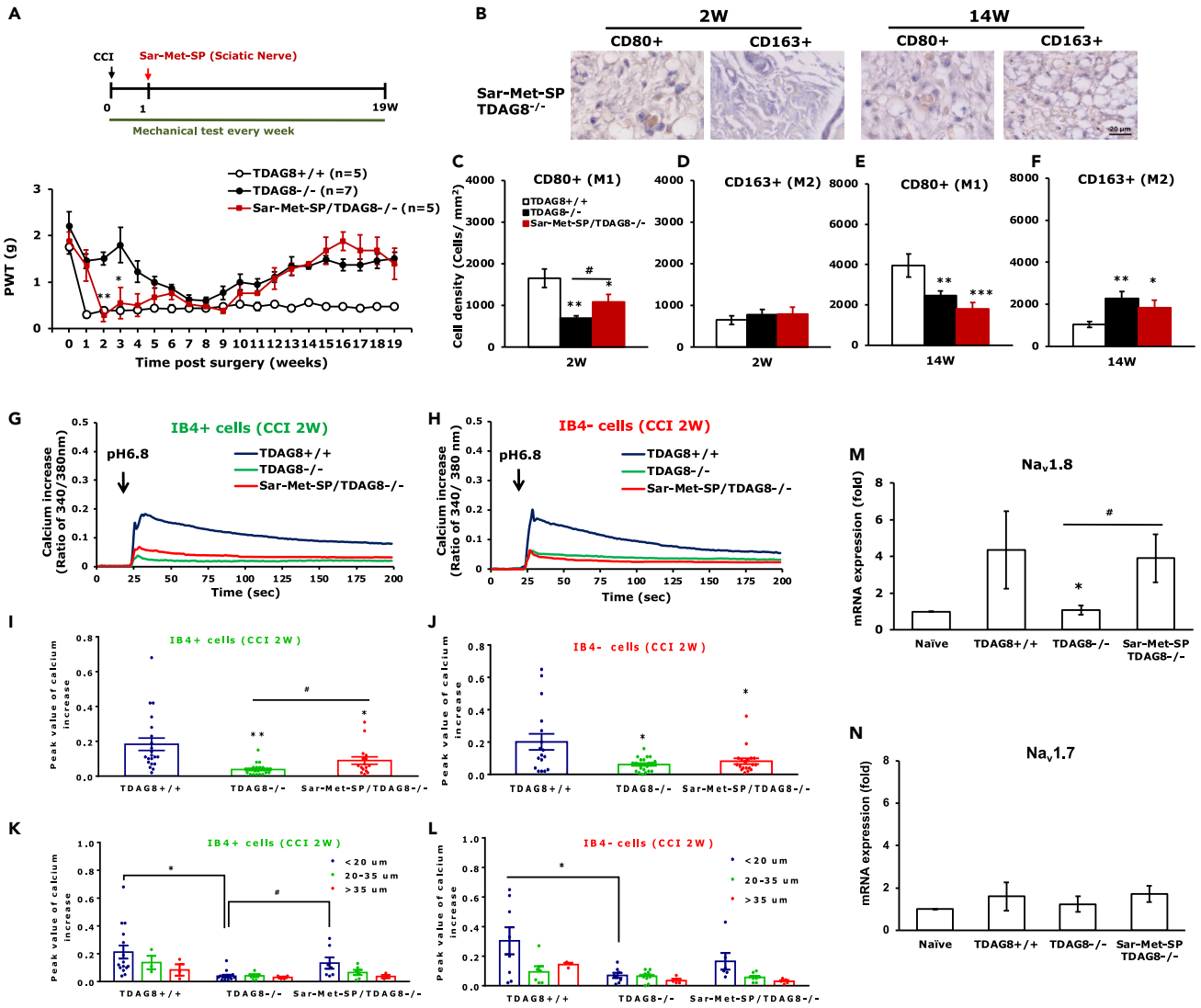

Figure 8. Substance P (SP) injection reverses TDAG8$^{-/-}$ attenuated mechanical allodynia in the early phase

(A) Sar-Met-SP (NK1 agonist) was locally delivered to the sciatic nerve (SN infiltration) of TDAG8$^{-/-}$ male mice at 1 week after CCI surgery. PWT was measured before (0 weeks) or at 1–19 weeks after surgery. Data are mean ± SEM of PWT. Sar-Met-SP/TDAG8$^{-/-}$ vs. TDAG8$^{-/-}$ at 1w $^{**}p = 0.008$; 2w $^{*}p = 0.042$ by two-way ANOVA with a post-hoc Bonferroni test.

(B–F) The sciatic nerve from the ipsilateral side of Sar-Met-SP–treated TDAG8$^{-/-}$ CCI male or female mice was excised at 2 and 14 weeks and the ligature was removed, cross-sectioned and immunostained with anti-CD80 or anti-CD163 antibodies. (B) Cell images from the sciatic nerve. Scale bar = 20 μm. (C–F) Cell density of CD80^{+} (C, E) or CD163^{+} (D, F) macrophages. Cell density was obtained by calculating the total cell number from a 1-mm^2 region. $n = 3$ for each treatment group. (C) TDAG8$^{+/+}$ vs. TDAG8$^{-/-}$ $p = 0.009$; TDAG8$^{+/+}$ vs. Sar-Met-SP/TDAG8$^{-/-}$ $p = 0.047$; TDAG8$^{-/-}$ vs. Sar-Met-SP/TDAG8$^{-/-}$ $p = 0.041$; (E) TDAG8$^{+/+}$ vs. TDAG8$^{-/-}$ $p = 0.009$; TDAG8$^{+/+}$ vs. Sar-Met-SP/TDAG8$^{-/-}$ $p < 0.001$; (F) TDAG8$^{+/+}$ vs. TDAG8$^{-/-}$ $p = 0.008$; TDAG8$^{+/+}$ vs. Sar-Met-SP/TDAG8$^{-/-}$ $p = 0.033$ by one-way ANOVA with a post-hoc Bonferroni test.

(G–N) Ipsilateral L4-6 DRG were taken from TDAG8$^{+/+}$, TDAG8$^{-/-}$ or Sar-Met-SP/TDAG8$^{-/-}$ male or female mice at 2 weeks after CCI surgery, then intracellular calcium signals (G–L) or gene expression (M, N) was detected. The time course of intracellular calcium signals is shown in G and H for IB4(+) or IB4(–) cells, respectively. (I, J) Mean ± SEM peak values of calcium signals in total neurons. TDAG8$^{+/+}$ vs. TDAG8$^{-/-}$ $^{**}p = 0.007$; TDAG8$^{+/+}$ vs. Sar-Met-SP/TDAG8$^{-/-}$ $^{*}p = 0.039$; TDAG8$^{-/-}$ vs. Sar-Met-SP/TDAG8$^{-/-}$ $\#p = 0.047$ by tone-way ANOVA with a post-hoc Bonferroni test. (J) Mean ± SEM peak values of calcium signals in total neurons. TDAG8$^{+/+}$ vs. TDAG8$^{-/-}$ $p = 0.031$; TDAG8$^{+/+}$ vs. Sar-Met-SP/TDAG8$^{-/-}$ $p = 0.043$ by one-way ANOVA with a post-hoc Bonferroni test. (K, L) Peak values for calcium signals of different populations of neurons. (K) TDAG8$^{+/+}$ $p = 0.021$; TDAG8$^{-/-}$vs. Sar-Met-SP/TDAG8$^{-/-}$ $p = 0.039$ by one-way ANOVA with a post-hoc Bonferroni test. (L) TDAG8$^{-/-}$ vs. TDAG8$^{+/+}$ $p = 0.038$ by one-way ANOVA with a post-hoc Bonferroni test. (M, N) Mean ± SEM fold change in $Na_v1.8$ (M) and $Na_v1.7$ (N) gene expression. $n = 3$ for each treatment group. $^{*}p = 0.048$ for TDAG8$^{+/+}$ vs. TDAG8$^{-/-}$; $\#p = 0.043$ for TDAG8$^{-/-}$ vs. Sar-Met-SP/TDAG8$^{-/-}$ by one-way ANOVA with a post-hoc Bonferroni test.

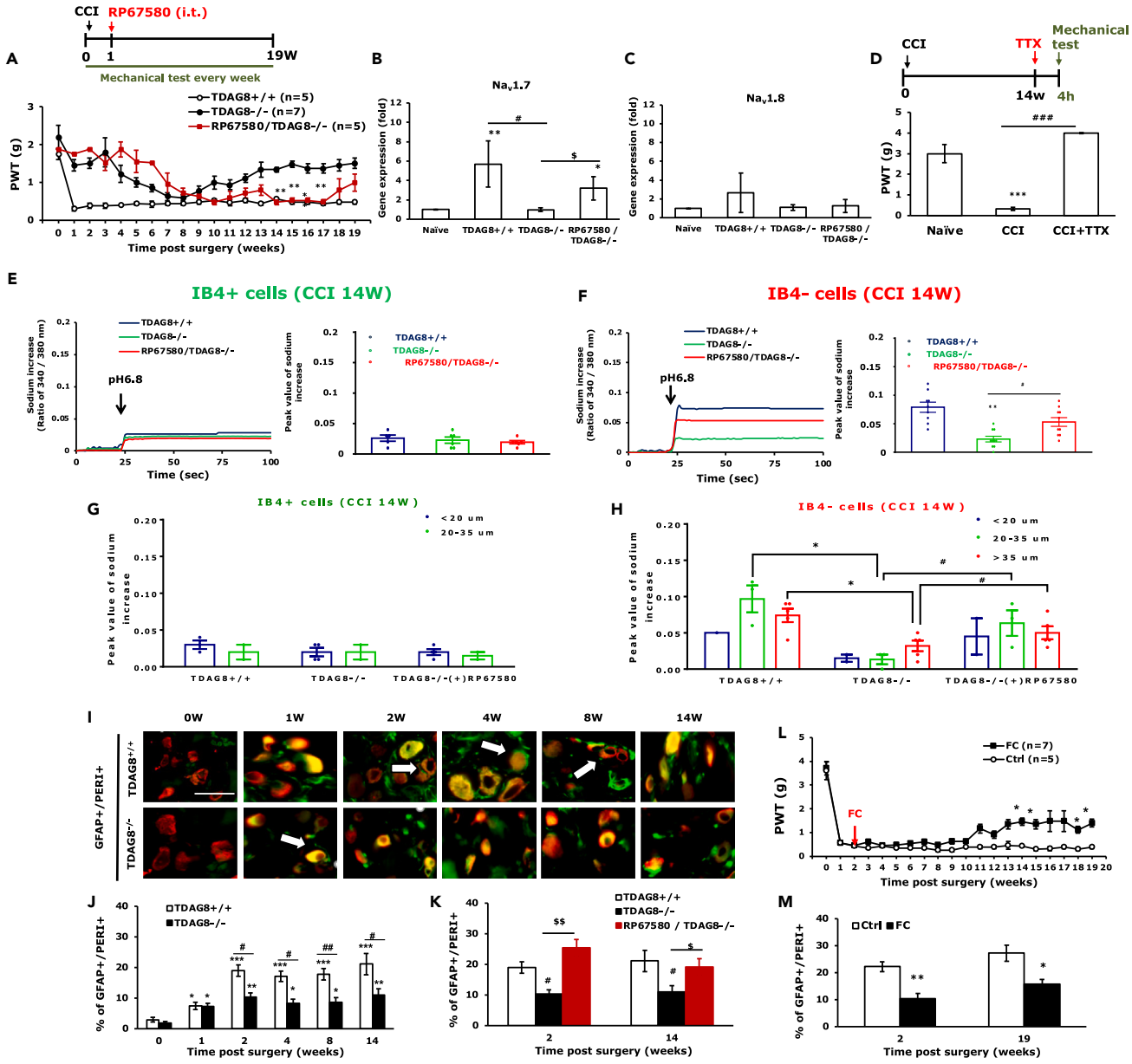

Figure 9. Administration of SP receptor antagonist reverses TDAG8$^{-/-}$ attenuated mechanical allodynia and a decline in satellite glial cell number in the late phase

(A) RP67580 (NK1 antagonist) was intrathecally injected into TDAG8$^{-/-}$ male mice at 1 week after CCI surgery. PWT was measured before (0 weeks) or 1–14 weeks after surgery. Data are mean ± SEM of PWT. $^{**}p = 0.006$ at 14-17w for RP67580/TDAG8$^{-/-}$ vs. TDAG8$^{-/-}$ mice by two-way ANOVA with a post-hoc Bonferroni test.

(B and C) Ipsilateral L4-6 DRG were taken from TDAG8$^{+/+}$, TDAG8$^{-/-}$ or RP67580/TDAG8$^{-/-}$ mice at 14 weeks after CCI surgery, then gene expression was detected. Mean ± SEM fold change of $Na_v1.7$ (B), and $Na_v1.8$ (C) gene expression. $n = 3$ male or female mice for each group. TDAG8$^{+/+}$ vs. naive $^{**}p = 0.005$, naive vs. RP67580/TDAG8$^{-/-}$ $^{*}p = 0.038$; TDAG8$^{+/+}$ vs. TDAG8$^{-/-}$ $\#p = 0.047$; $\$p = 0.043$ for TDAG8$^{-/-}$ vs. RP67580/TDAG8$^{-/-}$ by two-way ANOVA with a post-hoc Bonferroni test.

(D) TTX was intraplanarly injected at 14 weeks after CCI, then mice underwent mechanical tests. $N = 6$ male mice for each group. $^{***}p < 0.001$ for CCI vs. naive; $\#\#\#p < 0.001$ for CCI vs. CCI+TTX by one-way ANOVA with a post-hoc Bonferroni test.

(E and F) The time course of intracellular sodium signals is shown in left panels of E, F for IB4(+) or IB4(–) cells, respectively. Right panels of E, F are Mean ± SEM peak values of sodium signals in total neurons. $^{**}p = 0.008$ for TDAG8$^{+/+}$ vs. TDAG8$^{-/-}$; $\#p = 0.045$ for TDAG8$^{-/-}$ vs. RP67580/TDAG8$^{-/-}$ by two-way ANOVA with a post-hoc Bonferroni test.

Figure 9. *Continued*

(G and H) Peak values for sodium signals of different populations of neurons. #$p = 0.033$ for 20–35 μm TDAG8$^{-/-}$ vs. 20–35 μm RP67580/TDAG8$^{-/-}$; #$p = 0.048$ for >35 μm TDAG8$^{-/-}$ vs. > 35 μm RP67580/TDAG8$^{-/-}$; *$p = 0.021$ for 20–35 μm TDAG8$^{+/+}$ vs. 20–35 μm TDAG8$^{-/-}$; *$p = 0.034$ for >35 μm TDAG8$^{+/+}$ vs. > 35 μm TDAG8$^{-/-}$ by two-way ANOVA with a post-hoc Bonferroni test.

(I–K) Ipsilateral L5 DRG were taken from TDAG8$^{+/+}$, TDAG8$^{-/-}$, or RP67580/TDAG8$^{-/-}$ mice at 0, 1, 2, 4, 8, 14 weeks after CCI surgery and immunostained with anti-GFAP and anti-PERI antibodies. $N = 3$ male or female mice for each group. (I) Neuron images showing green fluorescence for GFAP(+) cells and red fluorescence for PERI(+) cells. (J) Mean ± SEM percentage of GFAP(+)/PERI(+) neurons in total PERI(+) neurons in TDAG8$^{+/+}$ and TDAG8$^{-/-}$ DRG. *$p = 0.034$ for 0w vs. 1w TDAG8$^{+/+}$; ***$p < 0.001$ for 0w vs. 2, 4, 8, 14w TDAG8$^{+/+}$; TDAG8$^{+/+}$ vs. TDAG8$^{-/-}$ at 2w #$p = 0.029$; 4w #$p = 0.033$; 8w ##$p = 0.009$; 14w #$p = 0.031$ by Z test. (K) The percentage of GFAP(+)/PERI(+) neurons in total PERI(+) neurons at 2 and 14 weeks in TDAG8$^{+/+}$, TDAG8$^{-/-}$, and RP67580/TDAG8$^{-/-}$ male or female mice. TDAG8$^{+/+}$ 2w vs. TDAG8$^{-/-}$ 2w #$p = 0.038$; TDAG8$^{+/+}$14w vs. TDAG8$^{-/-}$14w #$p = 0.038$; RP67580/TDAG8$^{-/-}$ 2w vs. TDAG8$^{-/-}$ 2w $$$p = 0.008$; RP67580/TDAG8$^{-/-}$ 14w vs. TDAG8$^{-/-}$ 14W $$p = 0.046$ by Z test.

(L and M) ICR male mice underwent CCI surgery, then the intrathecal administration of 1 nmol satellite glial cells (SGC) inhibitor, fluorocitric acid (FC) or vehicle at week 2. (L) Behavioral tests were performed for mechanical stimuli before (0 weeks) or at 1–19 weeks after CCI surgery. Data are mean ± SEM of PWT. $N = 7$ male mice for FC and $n = 5$ male mice for the control group. FC vs. Ctrl at 14w $p = 0.041$; 15w $p = 0.039$; 18w $p = 0.043$; 19w $p = 0.041$ by one-way ANOVA with a post-hoc Bonferroni test. (M) The percentage of GFAP(+)/PERI(+) neurons in total PERI(+) neurons at 2 and 19 weeks in Ctrl and FC-treated mice. $n = 3$ male or female mice for each group. FC and Ctrl at 2w **$p = 0.008$; 19w *$p = 0.037$ by Z test.

involved in CCI-induced mechanical allodynia in the first 2 weeks; it regulated the calcium and sodium signals in IB4(+) neurons and was co-expressed with TDAG8 or $Na_v1.8$ (Figures 4C, 4D, 4E, 4H, and 4I). Alternatively, TDAG8-induced cAMP could also activate PKA to further sensitize $Na_v1.8$ or increase $Na_v1.8$ expression, thereby enhancing $Na_v1.8$ function.[10] We found that blocking PKA attenuated mechanical allodynia at weeks 3 and 4 post-CCI. Although PKA did not directly influence the mechanical allodynia, we cannot exclude the PKA regulation of $Na_v1.8$ function or expression in the first 2 weeks. Thus, TDAG8-increased cAMP induces 1) short-term regulation by activating HCN to trigger $Na_v1.8$ activation, thereby initiating mechanical allodynia and 2) long-term regulation by activating PKA to regulate the expression and function of $Na_v1.8$ or other downstream pain-related molecules, thereby modulating the continuation of mechanical allodynia.

Although IB4(+) neurons are essential to trigger mechanical allodynia, IB4(−) neurons also have some role in early mechanical allodynia because the deletion of TDAG8 or pharmacological blockage of $Na_v1.8$ abolished calcium and sodium signals in both IB4(+) and IB4(−) small-diameter (<20 μm) neurons. TDAG8 activation in small-diameter IB4(−) neurons activates adenylyl cyclase to generate cAMP, then activate PKA. PKA activation contributes to SP release by the phosphorylation of N-methyl-D-aspartate receptor and voltage-gated calcium channels.[46] TDAG8-cAMP-PKA signaling may also upregulate $Na_v1.8$ channel expression or enhance $Na_v1.8$ function, which could generate high-frequency action potentials to activate voltage-gated calcium channels and induce calcium influx. Calcium influx triggers SP release in the periphery, in soma, and in the central site (spinal cord) of mice.

In the periphery, SP enhances the recruitment of immune cells and inflammation, thus facilitating mechanical allodynia. Reduction of M1 macrophage number by a macrophage blocker partially relieved mechanical allodynia (Figures 7F–7H), supporting the participation of M1 macrophages in mechanical allodynia. Peripheral delivery of SP reversed the analgesic effect induced by TDAG8 deletion on early mechanical allodynia. It also restored the TDAG8 deletion-suppressed increase in M1 macrophage number, $Na_v1.8$ expression, and small-diameter IB4(+) neuron activity (Figures 8C, 8K, and 8L).

In the spinal cord, SP released from the central terminal of IB4(−) primary afferents is responsible for the continuation of mechanical allodynia. Up-regulation of $Na_v1.8$ expression at 2w explained increased neuronal excitability (Figures 2E and 2F, 3A).[32,47] TDAG8-cAMP signaling-regulated SP release in the spinal cord further sensitizes spinal neurons and enhances nociceptive signals, contributing to the maintenance of mechanical allodynia.

T cell death-associated gene 8mediates IB4(−) neuron activity to maintain the late state of mechanical allodynia

Previous studies in inflammatory pain and muscle pain suggested an analgesic effect of SP.[48,49] We also found that the SP action on the DRG soma in the late phase is analgesic. The analgesic effect of SP observed in the late phase (>14 weeks) is not likely attributed to the action of the SP metabolic fragment, amino-terminal heptapeptide (SP_{1-7}), because SP_{1-7} provides an analgesic effect probably via binding unidentified molecular targets.[50] Nevertheless, the intrathecal administration of the NK1 antagonist reversed the analgesic effect induced by TDAG8 deletion in the late phase (Figure 9A), suggesting that the SP analgesic effect requires the NK1 receptor and is regulated by TDAG8. The analgesic effect of SP in inflammatory pain is attributed to opioid release at the peripheral level via immune cells or at the supraspinal level via neurons, and SP-opioid analgesia is mediated exclusively by the NK1 receptor.[51–54] SP-mediated analgesia in muscle pain seems to act on the potassium channel (M channel) to cause the hyperpolarization of neurons.[14] With SP delivered early at week 1 after CCI, the analgesic effect did not appear until 14 weeks (Figure 9A). The results agreed with the pharmacological blocking of SGCs, in which the blocker was administered early at week 2 but the analgesic effect appeared in the late phase of mechanical allodynia (Figure 9H).

The number of small-diameter DRG neurons surrounded by SGCs was increased over time after CCI, consistent with a previous study of L4 spinal nerve ligation.[14] TDAG8 deletion suppressed the increased number of SGCs from weeks 2–14. Such reduction seems related more to the maintenance of a late state of mechanical allodynia. Given that blocking the NK1 receptor reversed TDAG8 deletion-reduced SGC number (Figure 9G) and SP can activate the potassium channel to induce neuron hyperpolarization,[21] TDAG8-mediated SP release in soma could act on the NK1 receptor on DRG neurons, which activates the potassium channel to reduce small-diameter neuron activity, further attenuating the activation of SGCs. Calcium signals were decreased in small-diameter (<20 μm) DRG neurons at 14 weeks after CCI (Figure 2H), which supports this hypothesis. However, the TDAG8-SP anti-nociceptive effect was not obvious in TDAG8$^{+/+}$ mice because TDAG8 also mediated

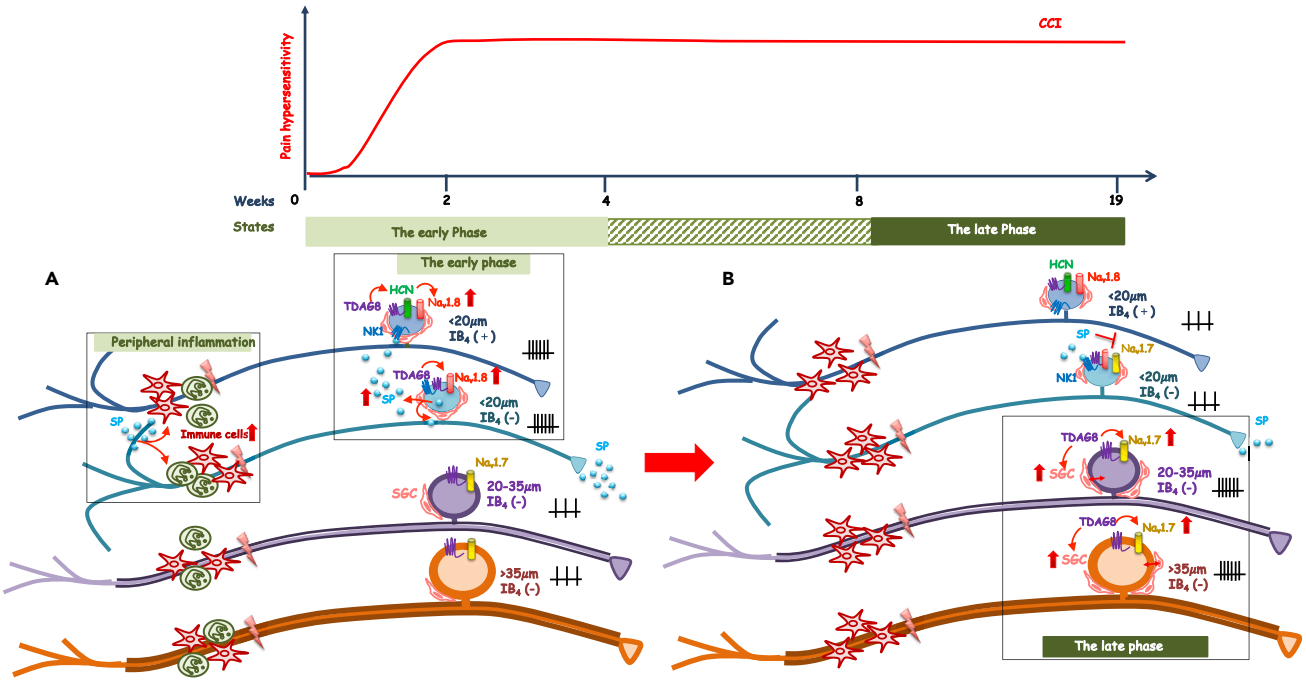

Figure 10. A putative model of the effect of TDAG8 modulation on the early and late phases of mechanical allodynia induced by nerve injury

(A) Activation of TDAG8 increases Na$_v$1.8 expression and modulates Na$_v$1.8 function in both IB4(+) and IB4(−) neurons, thus triggering the early phase of mechanical allodynia. In <20-μm diameter IB4(+) neurons, TDAG8 accumulates cAMP, which could activate HCN to modulate Na$_v$1.8 signaling, transducing nociceptive signals. In <20-μm diameter IB4(−) neurons, TDAG8 activation modulates Na$_v$1.8 function to release SP. SP increases Na$_v$1.8 expression and IB4(+) neuron activity; SP also acts on the periphery for recruiting immune cells, facilitating inflammation, and promoting the development of the early phase of mechanical allodynia.

(B) TDAG8 modulates SP release in soma to reduce SGC number, small-diameter neuron activity, and Na$_v$1.7 expression, thereby regulating the development of the late phase of mechanical allodynia. TDAG8 activation also increases medium-to large-diameter IB4(−) neuron activity, to facilitate the establishment and maintenance of the late state of mechanical allodynia. SGC, satellite glial cell.

a pro-nociceptive effect by increasing the activity of medium-to large-diameter (>20 μm) DRG neurons to overcome the TDAG8-SP anti-nociceptive effect, thus facilitating the development of the chronic phase. The TDAG8-SP anti-nociceptive and pro-nociceptive actions are both a "brake" and an "accelerator" for "stop" versus "go" functional regulation. This functions as a switch to promote the development of the chronic phase of mechanical allodynia.

Small-diameter neurons may release SP in trigeminal ganglia to increase NK1 expression in Aβ large neurons and increase Aβ large neuron activity, thus contributing to the mechanical allodynia induced by temporomandibular joint inflammation.[12,13] Similarly, we observed an increase in calcium level in medium-to large-diameter IB4(−) DRG neurons at 14 weeks after CCI; the increase was inhibited by TDAG8 deletion, suggesting that TDAG8-mediated increase in medium-to large-diameter neuron activity facilitates the development of late mechanical allodynia. As suggested by Li and Zhou[55] in L5 spinal injury, the sprouting axons of IB4(+) neurons are intermingled with IB4(+) satellite cells from the perineuronal ring structure surrounding large neurons, thereby regulating large-diameter neuron activity later after injury. Some small-diameter neurons also start to express GFAP. We observed GFAP expression in some small-diameter neurons in the late phase, which implies that a similar scenario could occur in the CCI model. After the injury, the central terminal IB4(−) neurons sprouting vigorously to the spinal cord[56] could contribute to maintaining mechanical allodynia.

IB4(−) neurons have a high density of TTX-sensitive (TTX-S) Na^+ currents[5,13]; large-diameter (>30 μm) DRG neurons preferentially express TTX-S sodium channels (Na$_v$1.1, Na$_v$1.6, Na$_v$1.7)[57]; and activated SGCs could also increase Na$_v$1.7 expression to promote Na$_v$1.7-involved mechanical hypernociception.[17] Na$_v$1.7 could play a role in mediating late mechanical allodynia. Selective deletion of Na$_v$1.7 in all DRG neurons but not in Na$_v$1.8-expressing neurons inhibits CCI-induced mechanical allodynia,[58] which suggests that Na$_v$1.7 in medium-to large-diameter neurons could be important for CCI-induced mechanical allodynia. As expected, pharmacological blockage of TTX-S channels inhibited the late phase of mechanical allodynia and increased Na$_v$1.7 expression at week 14 after CCI was inhibited by TDAG8 deletion; also, TDAG8 deletion-inhibited Na$_v$1.7 expression was reversed by NK1 antagonist treatment (Figures 9B, 9D, and 9G). Accordingly, TDAG8 likely mediates large-diameter IB4(−) DRG neuron activity by regulating Na$_v$1.7, thus contributing to the late phase of mechanical allodynia.

TDAG8-cAMP signaling regulates the early (1-4w) and the late (>13w) phase of mechanical allodynia. However, it remains unsolved why the mechanical threshold declined 5–12 weeks and which factors mediated the decline. Since tissue acidosis is still a trigger for mechanical allodynia, it would expect other proton-sensing receptors to be the candidates to regulate this 5-12 week period. It is partially attributed to

ASIC3 because ASIC3 deletion reverses CCI-induced mechanical allodynia from week 8.[29] However, we cannot exclude other non-proton-sensing receptors or factors involved in 5-12w regulation. It has been suggested that $Na_v1.8$ expression is up-regulated in uninjured neurons in the beginning of neuropathic pain but the upregulated expression is shifted to injured neurons.[47] The time-dependent shift in the $Na_v1.8$ function could also be a factor.

Limitations of the study

This study has uncovered that TDAG8 activation in small-diameter neurons modulates Nav1.8 signals in the early phase, while TDAG8 activation in medium-to-large diameter neurons modulates signals of TTX-S sodium channels in the late phase. A limitation of the study is that we only used neuron size to indicate the population of medium-to-large diameter neurons. Therefore, future studies need to address which population is responsible for the late phase of mechanical allodynia. Finding suitable markers for medium- or large-diameter neurons is essential to perform the ablation of specific populations for behavioral studies.

RESOURCE AVAILABILITY

Lead contact

Further information and requests for resources and reagents should be directed to and will be fulfilled by the Lead Contact, Wei-Hsin Sun (weihsin@nycu.edu.tw).

Materials availability

This study did not generate new unique reagents.

Data and code availability

- All data supporting the findings of this study are included as a Source Data file but can also be shared by the lead contact Wei-Hsin Sun upon request.
- No original code has been generated in this study.
- Any additional information required to reanalyze the data reported in this paper is available from the lead contact upon request.

ACKNOWLEDGMENTS

We thank the Taiwan Mouse Clinic, Academia Sinica, and Taiwan Animal Consortium for technical support in H&E staining. This work was supported by funds from the Ministry of Science and Technology (MOST), Taiwan (MOST 109-2320-B-010-027-MY3, MOST 111-2320-B-A49-011-MY3). Graphic abstract was created with BioRender.com.

AUTHOR CONTRIBUTIONS

SPD participated in the experimental design and performed animal and cell-based experiments and article writing. CCY participated in $Na_v1.8$ and IB4(+) animal experiments and immunostaining of TDAG8 and other proteins. Both SPD and CCY contribute equally. YC performed immunostaining of TDAG8 and other proteins. WHS conceived the study; participated in its design, coordination, and data interpretation; and contributed to writing the article. The graphic abstract is created with BioRender.com.

DECLARATION OF INTERESTS

The authors declare no conflicts of interest.

STAR★METHODS

Detailed methods are provided in the online version of this paper and include the following:

SUPPLEMENTAL INFORMATION

Supplemental information can be found online at https://doi.org/10.1016/j.isci.2024.110955.

Received: November 6, 2023
Revised: May 1, 2024

Accepted: September 10, 2024
Published: September 13, 2024

REFERENCES

1. Jensen, T.S., Baron, R., Haanpää, M., Kalso, E., Loeser, J.D., Rice, A.S.C., and Treede, R.D. (2011). A new definition of neuropathic pain. Pain *152*, 2204–2205. https://doi.org/10.1016/j.pain.2011.06.017.
2. Calvo, M., Dawes, J.M., and Bennett, D.L.H. (2012). The role of the immune system in the generation of neuropathic pain. Lancet Neurol. *11*, 629–642. https://doi.org/10.1016/S1474-4422(12)70134-5.
3. Ellis, A., and Bennett, D.L.H. (2013). Neuroinflammation and the generation of neuropathic pain. Br. J. Anaesth. *111*, 26–37. https://doi.org/10.1093/bja/aet128.
4. Richner, M., Ulrichsen, M., Elmegaard, S.L., Dieu, R., Pallesen, L.T., and Vaegter, C.B. (2014). Peripheral nerve injury modulates neurotrophin signaling in the peripheral and central nervous system. Mol. Neurobiol. *50*, 945–970. https://doi.org/10.1007/s12035-014-8706-9.
5. Ueda, H. (2006). Molecular mechanisms of neuropathic pain-phenotypic switch and initiation mechanisms. Pharmacol. Ther. *109*, 57–77. https://doi.org/10.1016/j.pharmthera.2005.06.003.
6. Huang, C.W., Tzeng, J.N., Chen, Y.J., Tsai, W.F., Chen, C.C., and Sun, W.H. (2007). Nociceptors of dorsal root ganglion express proton-sensing G-protein-coupled receptors. Mol. Cell. Neurosci. *36*, 195–210. https://doi.org/10.1016/j.mcn.2007.06.010.
7. Sacerdote, P., Franchi, S., Trovato, A.E., Valsecchi, A.E., Panerai, A.E., and Colleoni, M. (2008). Transient early expression of TNF-alpha in sciatic nerve and dorsal root ganglia in a mouse model of painful peripheral neuropathy. Neurosci. Lett. *436*, 210–213. https://doi.org/10.1016/j.neulet.2008.03.023.
8. Shamash, S., Reichert, F., and Rotshenker, S. (2002). The cytokine network of Wallerian degeneration: tumor necrosis factor-alpha, interleukin-1alpha, and interleukin-1beta. J. Neurosci. *22*, 3052–3060. https://doi.org/10.1523/JNEUROSCI.22-08-03052.2002.
9. Chen, Y.J., Huang, C.W., Lin, C.S., Chang, W.H., and Sun, W.H. (2009). Expression and function of proton-sensing G-protein-coupled receptors in inflammatory pain. Mol. Pain *5*, 39. https://doi.org/10.1186/1744-8069-5-39.
10. Gold, M.S., Levine, J.D., and Correa, A.M. (1998). Modulation of TTX-R INa by PKC and PKA and their role in PGE2-induced sensitization of rat sensory neurons in vitro. J. Neurosci. *18*, 10345–10355. https://doi.org/10.1523/JNEUROSCI.18-24-10345.1998.
11. Chiu, I.M., von Hehn, C.A., and Woolf, C.J. (2012). Neurogenic inflammation and the peripheral nervous system in host defense and immunopathology. Nat. Neurosci. *15*, 1063–1067. https://doi.org/10.1038/nn.3144.
12. Takeda, M., Tanimoto, T., Nasu, M., Ikeda, M., Kadoi, J., and Matsumoto, S. (2005). Activation of NK1 receptor of trigeminal root ganglion via substance P paracrine mechanism contributes to the mechanical allodynia in the temporomandibular joint inflammation in rats. Pain *116*, 375–385. https://doi.org/10.1016/j.pain.2005.05.007.
13. Takeda, M., Tanimoto, T., Ikeda, M., Nasu, M., Kadoi, J., Shima, Y., Ohta, H., and Matsumoto, S. (2005). Temporomandibular joint inflammation potentiates the excitability of trigeminal root ganglion neurons innervating the facial skin in rats. J. Neurophysiol. *93*, 2723–2738. https://doi.org/10.1152/jn.00631.2004.
14. Lin, C.C.J., Chen, W.N., Chen, C.J., Lin, Y.W., Zimmer, A., and Chen, C.C. (2012). An antinociceptive role for substance P in acid-induced chronic muscle pain. Proc. Natl. Acad. Sci. USA *109*, E76–E83. https://doi.org/10.1073/pnas.1108903108.
15. Costa, F.A.L., and Moreira Neto, F.L. (2015). [Satellite glial cells in sensory ganglia: its role in pain]. Rev. Bras. Anestesiol. *65*, 73–81. https://doi.org/10.1016/j.bjan.2013.07.013.
16. Huang, L.Y.M., Gu, Y., and Chen, Y. (2013). Communication between neuronal somata and satellite glial cells in sensory ganglia. Glia *61*, 1571–1581. https://doi.org/10.1002/glia.22541.
17. Jin, Y.Z., Zhang, P., Hao, T., Wang, L.M., Guo, M.D., and Gan, Y.H. (2019). Connexin 43 contributes to temporomandibular joint inflammation induced-hypernociception via sodium channel 1.7 in trigeminal ganglion. Neurosci. Lett. *707*, 134301. https://doi.org/10.1016/j.neulet.2019.134301.
18. Okajima, F. (2013). Regulation of inflammation by extracellular acidification and proton-sensing GPCRs. Cell. Signal. *25*, 2263–2271. https://doi.org/10.1016/j.cellsig.2013.07.022.
19. Poirot, O., Berta, T., Decosterd, I., and Kellenberger, S. (2006). Distinct ASIC currents are expressed in rat putative nociceptors and are modulated by nerve injury. J. Physiol. *576*, 215–234. https://doi.org/10.1113/jphysiol.2006.113035.
20. Reeh, P.W., and Steen, K.H. (1996). Tissue acidosis in nociception and pain. Prog. Brain Res. *113*, 143–151. https://doi.org/10.1016/s0079-6123(08)61085-7.
21. Ishii, S., Kihara, Y., and Shimizu, T. (2005). Identification of T cell death-associated gene 8 (TDAG8) as a novel acid sensing G-protein-coupled receptor. J. Biol. Chem. *280*, 9083–9087. https://doi.org/10.1074/jbc.M407832200.
22. Wang, J.Q., Kon, J., Mogi, C., Tobo, M., Damirin, A., Sato, K., Komachi, M., Malchinkhuu, E., Murata, N., Kimura, T., et al. (2004). TDAG8 is a proton-sensing and psychosine-sensitive G-protein-coupled receptor. J. Biol. Chem. *279*, 45626–45633. https://doi.org/10.1074/jbc.M406966200.
23. Dai, S.P., Huang, Y.H., Chang, C.J., Huang, Y.F., Hsieh, W.S., Tabata, Y., Ishii, S., and Sun, W.H. (2017). TDAG8 involved in initiating inflammatory hyperalgesia and establishing hyperalgesic priming in mice. Sci. Rep. *7*, 41415. https://doi.org/10.1038/srep41415.
24. Hsieh, W.S., Kung, C.C., Huang, S.L., Lin, S.C., and Sun, W.H. (2017). TDAG8, TRPV1, and ASIC3 involved in establishing hyperalgesic priming in experimental rheumatoid arthritis. Sci. Rep. *7*, 8870. https://doi.org/10.1038/s41598-017-09200-6.
25. Kung, C.C., Dai, S.P., Chiang, H., Huang, H.S., and Sun, W.H. (2020). Temporal expression patterns of distinct cytokines and M1/M2 macrophage polarization regulate rheumatoid arthritis progression. Mol. Biol. Rep. *47*, 3423–3437. https://doi.org/10.1007/s11033-020-05422-6.
26. Jin, Y., Sato, K., Tobo, A., Mogi, C., Tobo, M., Murata, N., Ishii, S., Im, D.S., and Okajima, F. (2014). Inhibition of interleukin-1beta production by extracellular acidification through the TDAG8/cAMP pathway in mouse microglia. J. Neurochem. *129*, 683–695. https://doi.org/10.1111/jnc.12661.
27. Mogi, C., Tobo, M., Tomura, H., Murata, N., He, X.D., Sato, K., Kimura, T., Ishizuka, T., Sasaki, T., Sato, T., et al. (2009). Involvement of proton-sensing TDAG8 in extracellular acidification-induced inhibition of proinflammatory cytokine production in peritoneal macrophages. J. Immunol. *182*, 3243–3251. https://doi.org/10.4049/jimmunol.0803466.
28. Onozawa, Y., Fujita, Y., Kuwabara, H., Nagasaki, M., Komai, T., and Oda, T. (2012). Activation of T cell death-associated gene 8 regulates the cytokine production of T cells and macrophages in vitro. Eur. J. Pharmacol. *683*, 325–331. https://doi.org/10.1016/j.ejphar.2012.03.007.
29. Kung, C.C., Huang, Y.C., Hung, T.Y., Teng, C.Y., Lee, T.Y., and Sun, W.H. (2020). Deletion of Acid-Sensing Ion Channel 3 Relieves the Late Phase of Neuropathic Pain by Preventing Neuron Degeneration and Promoting Neuron Repair. Cells-Basel *9*, 2355. https://doi.org/10.3390/cells9112355.
30. Huang, Y.H., Su, Y.S., Chang, C.J., and Sun, W.H. (2016). Heteromerization of G2A and OGR1 enhances proton sensitivity and proton-induced calcium signals. J. Recept. Signal Transduct. Res. *36*, 633–644. https://doi.org/10.3109/10799893.2016.1155064.
31. Dai, S.P., Hsieh, W.S., Chen, C.H., Lu, Y.H., Huang, H.S., Chang, D.M., Huang, S.L., and Sun, W.H. (2020). TDAG8 deficiency reduces satellite glial number and pro-inflammatory macrophage number to relieve rheumatoid arthritis disease severity and chronic pain. J. Neuroinflammation *17*, 170. https://doi.org/10.1186/s12974-020-01851-z.
32. Faber, C.G., Lauria, G., Merkies, I.S.J., Cheng, X., Han, C., Ahn, H.S., Persson, A.K., Hoeijmakers, J.G.J., Gerrits, M.M., Pierro, T., et al. (2012). Gain-of-function Nav1.8 mutations in painful neuropathy. Proc. Natl. Acad. Sci. USA *109*, 19444–19449. https://doi.org/10.1073/pnas.1216080109.
33. Pinto, L.G., Souza, G.R., Kusuda, R., Lopes, A.H., Sant'Anna, M.B., Cunha, F.Q., Ferreira, S.H., and Cunha, T.M. (2019). Non-Peptidergic Nociceptive Neurons Are Essential for Mechanical Inflammatory Hypersensitivity in Mice. Mol. Neurobiol. *56*, 5715–5728. https://doi.org/10.1007/s12035-019-1494-5.
34. Hamilton, J.A., and Tak, P.P. (2009). The dynamics of macrophage lineage populations in inflammatory and autoimmune diseases. Arthritis Rheum. *60*, 1210–1221. https://doi.org/10.1002/art.24505.
35. Stucky, C.L., and Lewin, G.R. (1999). Isolectin B(4)-positive and -negative nociceptors are functionally distinct. J. Neurosci. *19*, 6497–

6505. https://doi.org/10.1523/JNEUROSCI.19-15-06497.1999.
36. Wu, Z.Z., and Pan, H.L. (2004). Tetrodotoxin-sensitive and -resistant Na+ channel currents in subsets of small sensory neurons of rats. Brain Res. *1029*, 251–258. https://doi.org/10.1016/j.brainres.2004.09.051.
37. Akopian, A.N., Sivilotti, L., and Wood, J.N. (1996). A tetrodotoxin-resistant voltage-gated sodium channel expressed by sensory neurons. Nature *379*, 257–262. https://doi.org/10.1038/379257a0.
38. Abrahamsen, B., Zhao, J., Asante, C.O., Cendan, C.M., Marsh, S., Martinez-Barbera, J.P., Nassar, M.A., Dickenson, A.H., and Wood, J.N. (2008). The cell and molecular basis of mechanical, cold, and inflammatory pain. Science *321*, 702–705. https://doi.org/10.1126/science.1156916.
39. Tarpley, J.W., Kohler, M.G., and Martin, W.J. (2004). The behavioral and neuroanatomical effects of IB4-saporin treatment in rat models of nociceptive and neuropathic pain. Brain Res. *1029*, 65–76. https://doi.org/10.1016/j.brainres.2004.09.027.
40. Lai, J., Gold, M.S., Kim, C.S., Bian, D., Ossipov, M.H., Hunter, J.C., and Porreca, F. (2002). Inhibition of neuropathic pain by decreased expression of the tetrodotoxin-resistant sodium channel, NaV1.8. Pain *95*, 143–152. https://doi.org/10.1016/s0304-3959(01)00391-8.
41. Jarvis, M.F., Honore, P., Shieh, C.C., Chapman, M., Joshi, S., Zhang, X.F., Kort, M., Carroll, W., Marron, B., Atkinson, R., et al. (2007). A-803467, a potent and selective Nav1.8 sodium channel blocker, attenuates neuropathic and inflammatory pain in the rat. Proc. Natl. Acad. Sci. USA *104*, 8520–8525. https://doi.org/10.1073/pnas.0611364104.
42. Ekberg, J., Jayamanne, A., Vaughan, C.W., Aslan, S., Thomas, L., Mould, J., Drinkwater, R., Baker, M.D., Abrahamsen, B., Wood, J.N., et al. (2006). muO-conotoxin MrVIB selectively blocks Nav1.8 sensory neuron specific sodium channels and chronic pain behavior without motor deficits. Proc. Natl. Acad. Sci. USA *103*, 17030–17035. https://doi.org/10.1073/pnas.0601819103.
43. Dong, X.W., Goregoaker, S., Engler, H., Zhou, X., Mark, L., Crona, J., Terry, R., Hunter, J., and Priestley, T. (2007). Small interfering RNA-mediated selective knockdown of Na(V)1.8 tetrodotoxin-resistant sodium channel reverses mechanical allodynia in neuropathic rats. Neuroscience *146*, 812–821. https://doi.org/10.1016/j.neuroscience.2007.01.054.
44. Blair, N.T., and Bean, B.P. (2002). Roles of tetrodotoxin (TTX)-sensitive Na+ current, TTX-resistant Na+ current, and Ca2+ current in the action potentials of nociceptive sensory neurons. J. Neurosci. *22*, 10277–10290. https://doi.org/10.1523/JNEUROSCI.22-23-10277.2002.
45. Emery, E.C., Young, G.T., Berrocoso, E.M., Chen, L., and McNaughton, P.A. (2011). HCN2 ion channels play a central role in inflammatory and neuropathic pain. Science *333*, 1462–1466. https://doi.org/10.1126/science.1206243.
46. Chen, W., McRoberts, J.A., Ennes, H.S., and Marvizon, J.C. (2021). cAMP signaling through protein kinase A and Epac2 induces substance P release in the rat spinal cord. Neuropharmacology *189*, 108533. https://doi.org/10.1016/j.neuropharm.2021.108533.
47. Coward, K., Plumpton, C., Facer, P., Birch, R., Carlstedt, T., Tate, S., Bountra, C., and Anand, P. (2000). Immunolocalization of SNS/PN3 and NaN/SNS2 sodium channels in human pain states. Pain *85*, 41–50. https://doi.org/10.1016/s0304-3959(99)00251-1.
48. Lin, S.Y., Chang, W.J., Lin, C.S., Huang, C.Y., Wang, H.F., and Sun, W.H. (2011). Serotonin receptor 5-HT2B mediates serotonin-induced mechanical hyperalgesia. J. Neurosci. *31*, 1410–1418. https://doi.org/10.1523/JNEUROSCI.4682-10.2011.
49. Parenti, C., Aricò, G., Ronsisvalle, G., and Scoto, G.M. (2012). Supraspinal injection of Substance P attenuates allodynia and hyperalgesia in a rat model of inflammatory pain. Peptides *34*, 412–418. https://doi.org/10.1016/j.peptides.2012.01.016.
50. Nyman, J., Guo, N., Sandström, A., Hallberg, M., Nyberg, F., and Yu, L. (2021). The amino-terminal heptapeptide of the algesic substance P provides analgesic effect in relieving chronic neuropathic pain. Eur. J. Pharmacol. *892*, 173820. https://doi.org/10.1016/j.ejphar.2020.173820.
51. Rittner, H.L., Mousa, S.A., Labuz, D., Beschmann, K., Schäfer, M., Stein, C., and Brack, A. (2006). Selective local PMN recruitment by CXCL1 or CXCL2/3 injection does not cause inflammatory pain. J. Leukoc. Biol. *79*, 1022–1032. https://doi.org/10.1189/jlb.0805452.
52. Rosén, A., Zhang, Y.X., Lund, I., Lundeberg, T., and Yu, L.C. (2004). Substance P microinjected into the periaqueductal gray matter induces antinociception and is released following morphine administration. Brain Res. *1001*, 87–94. https://doi.org/10.1016/j.brainres.2003.11.060.
53. Improta, G., and Broccardo, M. (2000). Effects of supraspinal administration of PG-SPI and PG-KII, two amphibian tachykinin peptides, on nociception in the rat. Peptides *21*, 1611–1616. https://doi.org/10.1016/s0196-9781(00)00292-8.
54. Brack, A., Rittner, H.L., Machelska, H., Leder, K., Mousa, S.A., Schäfer, M., and Stein, C. (2004). Control of inflammatory pain by chemokine-mediated recruitment of opioid-containing polymorphonuclear cells. Pain *112*, 229–238. https://doi.org/10.1016/j.pain.2004.08.029.
55. Li, L., and Zhou, X.F. (2001). Pericellular Griffonia simplicifolia I isolectin B4-binding ring structures in the dorsal root ganglia following peripheral nerve injury in rats. J. Comp. Neurol. *439*, 259–274. https://doi.org/10.1002/cne.1349.
56. Belyantseva, I.A., and Lewin, G.R. (1999). Stability and plasticity of primary afferent projections following nerve regeneration and central degeneration. Eur. J. Neurosci. *11*, 457–468. https://doi.org/10.1046/j.1460-9568.1999.00458.x.
57. Ho, C., and O'Leary, M.E. (2011). Single-cell analysis of sodium channel expression in dorsal root ganglion neurons. Mol. Cell. Neurosci. *46*, 159–166. https://doi.org/10.1016/j.mcn.2010.08.017.
58. Minett, M.S., Falk, S., Santana-Varela, S., Bogdanov, Y.D., Nassar, M.A., Heegaard, A.M., and Wood, J.N. (2014). Pain without nociceptors? Nav1.7-independent pain mechanisms. Cell Rep. *6*, 301–312. https://doi.org/10.1016/j.celrep.2013.12.033.
59. Bu, L., Gao, M., Qu, S., and Liu, D. (2013). Intraperitoneal injection of clodronate liposomes eliminates visceral adipose macrophages and blocks high-fat diet-induced weight gain and development of insulin resistance. AAPS J. *15*, 1001–1011. https://doi.org/10.1208/s12248-013-9501-7.
60. Huang, W.Y., Dai, S.P., Chang, Y.C., and Sun, W.H. (2015). Acidosis Mediates the Switching of Gs-PKA and Gi-PKCepsilon Dependence in Prolonged Hyperalgesia Induced by Inflammation. PLoS One *10*, e0125022. https://doi.org/10.1371/journal.pone.0125022.
61. Emonds-Alt, X., Doutremepuich, J.D., Heaulme, M., Neliat, G., Santucci, V., Steinberg, R., Vilain, P., Bichon, D., Ducoux, J.P., Proietto, V., et al. (1993). In vitro and in vivo biological activities of SR140333, a novel potent non-peptide tachykinin NK1 receptor antagonist. Eur. J. Pharmacol. *250*, 403–413. https://doi.org/10.1016/0014-2999(93)90027-f.
62. Bassi, G.S., de Carvalho, M.C., and Brandão, M.L. (2014). Effects of substance P and Sar-Met-SP, a NK1 agonist, in distinct amygdaloid nuclei on anxiety-like behavior in rats. Neurosci. Lett. *569*, 121–125. https://doi.org/10.1016/j.neulet.2014.03.065.
63. Chapman, V., and Dickenson, A.H. (1993). The effect of intrathecal administration of RP67580, a potent neurokinin 1 antagonist on nociceptive transmission in the rat spinal cord. Neurosci. Lett. *157*, 149–152. https://doi.org/10.1016/0304-3940(93)90724-y.
64. Chung, E., Yoon, T.G., Kim, S., Kang, M., Kim, H.J., and Son, Y. (2017). Intravenous Administration of Substance P Attenuates Mechanical Allodynia Following Nerve Injury by Regulating Neuropathic Pain-Related Factors. Biomol. Ther. *25*, 259–265. https://doi.org/10.4062/biomolther.2016.137.
65. Su, Y.S., Mei, H.R., Wang, C.H., and Sun, W.H. (2018). Peripheral 5-HT(3) mediates mirror-image pain by a cross-talk with acid-sensing ion channel 3. Neuropharmacology *130*, 92–104. https://doi.org/10.1016/j.neuropharm.2017.11.044.
66. Pearson, E.S., Pearson, E.S., Hartley, H.O., and Pearson, K. (1976). Biometrika Tables for Statisticians, 3nd ed., Reprinted with Corrections, Edition (Biometrika Trust) (JSTOR).

STAR★METHODS

KEY RESOURCES TABLE

REAGENT or RESOURCE	SOURCE	IDENTIFIER
Antibodies		
Rabbit polyclonal anti-CD80	Biorbyt	Cat#: ORB5805; NA
Rabbit polyclonal anti-CD163	Biorbyt	Cat#: ORB13303; NA
Mouse monoclonal anti-peripherin	Sigma-Aldrich	Cat#: P5117; RRID: AB_477360
Rabbit polyclonal anti-glial fibrillary acidic protein	Dako, Santa Clara	Cat#: Z033401; NA
Mouse monoclonal anti-calcitonin gene related peptide	Santa Cruz	Cat#: sc-57053; NA
Isolectin B4, FITC conjugate	Sigma	Cat#: L2895; NA
Mouse monoclonal anti-neurofilament	Sigma	Cat#: N0142; RRID: AB_477257
Rabbit polyclonal anti-fatty acid binding protein 7	Proteintech	Cat#: 51010-1-AP; NA
Rabbit polyclonal anti-TDAG8	Genesis	Customization; NA
TRITC-conjugated goat anti-mouse IgG	Sigma-Aldrich	Cat#: T5393; NA
FITC-conjugated goat anti-rabbit IgG	Sigma-Aldrich	Cat#: F0382; NA
FITC-conjugated goat anti-mouse IgG	Sigma-Aldrich	Cat#: F9006; NA
Chemicals, peptides, and recombinant proteins		
Fura-2-AM Dye	Thermo Fisher	Cat#: 65-0858-39
SBFI, AM	Thermo Fisher	Cat#: S1263
RP67580 (Neurokinin-1 receptor antagonist)	Tocris Bioscience	Cat#: 1635
[Sar9, Met(O2)11] (Sar-Met-SP)	Tocris Bioscience	Cat#: 1178/1
H89 dihydrochloride	Tocris Bioscience	Cat#: 2910/1
Tetrodotoxin (TTX)	Tocris Bioscience	Cat#: 1078/1
Clodronate-liposome	LIPOSOMA	SKU: C-005
IB4-saporin (IB4-SAP)	ATSbio	Cat#: KIT-10
A803467	TargetMol	Cat#: T2024
ZD7288 (HCN channel blocker)	MedChemExpress	Cat#: HY-101346
DL-Fluorocitric acid barium salt	Sigma-Adrich	Cat#: F9634
NSC745885	Kung et al.[25]	https://pubmed.ncbi.nlm.nih.gov/32277445/
PcTx1 (Psalmotoxin 1, ASIC1a blocker)	Tocris Bioscience	Cat#: 5042
APETx2 (ASIC3 blocker)	Alomone Labs	Cat#: RTA-100
HC030031 (TRPA1 blocker)	MedChemExpress	Cat#: HY-15064
Capsazepine (TRPV1 blocker)	Tocris Bioscience	Cat#: 0464
Critical commercial assays		
cAMP immunoassay kit	R&D systems	Cat#: QC53
RNeasy kit	Qiagen	Cat#: 74004
tumor necrosis factor α (TNF-α) kit	R&D systems	Cat#: MTA00B
interleukin 6 (IL-6) kit	R&D systems	Cat#: M6000B
interleukin 10 (IL-10) kit	R&D systems	Cat#: M1000B
Experimental models: Organisms/strains		
Mouse: Crl:CD1(ICR)	BioLASCO	Cat#: LAAICRB1H
Mouse: C57BL/6 (TDAG8$^{+/+}$ and TDAG8$^{-/-}$)	Dai et al.[31]	https://pubmed.ncbi.nlm.nih.gov/32471455/

(*Continued on next page*)

Continued

REAGENT or RESOURCE	SOURCE	IDENTIFIER
Mouse: ICR (TRPV1$^{+/+}$ and TRPV1$^{-/-}$)	Hsieh et al.[24]	https://www.nature.com/articles/s41598-017-09200-6
Oligonucleotides		
RT Primer: TDAG8 Forward: ATAGTCAGCGTCCCAGCCACC	Hsieh et al.[24]	https://www.nature.com/articles/s41598-017-09200-6
RT Primer: TDAG8 Reverse: CGCTTCCTTTGCACAAGGTG	Hsieh et al.[24]	https://www.nature.com/articles/s41598-017-09200-6
RT Primer: $Na_v1.7$ Forward: CAACGCACTCATAGGAGCAA	This paper	N/A
RT Primer: $Na_v1.7$ Reverse: CTTGCCAGCAAACAGATTGAC	This paper	N/A
RT Primer: $Na_v1.8$ Forward: GTAGTGGTGGATGCCTTGGT	This paper	N/A
RT Primer: $Na_v1.8$ Reverse: AAGTGGCCGGTATTGTTTTG	This paper	N/A
RT Primer: TRPV1 Forward: TCTCCACTGGTGTTGAGACG	Hsieh et al.[24]	https://www.nature.com/articles/s41598-017-09200-6
RT Primer: TRPV1 Reverse: GGGTCTTTGAACTCGCTGTC	Hsieh et al.[24]	https://www.nature.com/articles/s41598-017-09200-6
RT Primer: ASIC3 Forward: TTTCACCTGTCTTGGCTCCT	Hsieh et al.[24]	https://www.nature.com/articles/s41598-017-09200-6
RT Primer: ASIC3 Reverse: CAGGATAGTGGTGGGGATTG	Hsieh et al.[24]	https://www.nature.com/articles/s41598-017-09200-6
Genotyping primer: TDAG8$^{-/-}$ Forward: GAACCATTAGTTTGGCTCATGTGACTG	Dai et al.[31]	https://link.springer.com/article/10.1186/s12974-020-01851-z
Genotyping primer: TDAG8$^{-/-}$ Reverse: CTTGTGTCATGCACAAAGTAGATGTCC	Dai et al.[31]	https://link.springer.com/article/10.1186/s12974-020-01851-z
Genotyping primer: TDAG8$^{+/+}$ Forward: CGAACTCTAGCTGGCTTTTATCCAATAAT	Dai et al.[31]	https://link.springer.com/article/10.1186/s12974-020-01851-z
Genotyping primer: TDAG8$^{+/+}$ Reverse: GAACCATTAGTTTGGCTCATGTGACTG	Dai et al.[31]	https://link.springer.com/article/10.1186/s12974-020-01851-z
Genotyping primer: TRPV1$^{-/-}$ Forward: CACGAGACTAGTGAGACGTG	Hsieh et al.[24]	https://www.nature.com/articles/s41598-017-09200-6
Genotyping primer: TRPV1$^{-/-}$ Reverse: TCCTCATGCACTTCAGGAAA	Hsieh et al.[24]	https://www.nature.com/articles/s41598-017-09200-6
Genotyping primer: TRPV1$^{+/+}$ Forward: CCTGCTCAACATGCTCATTG	Hsieh et al.[24]	https://www.nature.com/articles/s41598-017-09200-6
Genotyping primer: TRPV1$^{+/+}$ Reverse: TCCTCATGCACTTCAGGAAA	Hsieh et al.[24]	https://www.nature.com/articles/s41598-017-09200-6
Software and algorithms		
MetaVue software	Major Instruments Co., Ltd.	http://www.major.com.tw/
Meta Fluor software	Major Instruments Co., Ltd.	http://www.major.com.tw/

EXPERIMENTAL MODEL AND STUDY PARTICIPANT DETAILS

Animals

Male and female ICR mice (8–12 weeks old) were purchased from BioLASCO Taiwan (Taipei) and housed 3–4 per cage under a 12-h light/dark cycle (lights on at 7:00) with food and water *ad libitum* in a temperature- and humidity-controlled environment at the National Yang Ming Chiao Tung University. The care and use of mice conformed to the Guide for the Use of Laboratory Animals (US National Research Council), and the experimental procedures were approved by the local animal use committee (IACUC, National Yang Ming Chiao Tung University,

Taiwan, IACUC numbers: 1080709; 1090223). All behavioral testing was performed between 9:00 and 17:00 h. Efforts were made to minimize the number of animals used and their suffering. For gene expression, histoimmunostaining, or primary culture, mice were placed in the euthanasia chamber and killed by introducing 100% CO_2. Dorsal root ganglia (DRG) or sciatic nerves were excised for RNA extraction, sectioning, or primary culture.

TDAG8$^{-/-}$ and TDAG8$^{+/+}$ mice were generated as described.[23] The genotyping primer sequences were for TDAG8$^{-/-}$, 5′-gaaccat tagtttggctcatgtgactg/5′-cttgtgtcatgcacaaagtagatgtcc, and for TDAG8$^{+/+}$, 5′-cgaactctagctggcttttatccaataat/5′-gaaccattagtttggctcatgt gactg. TRPV1$^{-/-}$ and TRPV1$^{+/+}$ mice on a CD1/ICR background are generated as described.[24] The genotyping primer sequences were for TRPV1$^{-/-}$, 5′-cacgagactagtgagacgtg/5′-tcctcatgcacttcaggaaa; and for TRPV1$^{+/+}$, 5′-cctgctcaacatgctcattg/5′-tcctcatgcacttcaggaaa.

Primary DRG culture

Primary DRG culture was performed as described.[9] Briefly, L4-6 DRG were isolated from TDAG8$^{+/+}$, TDAG8$^{-/-}$, or Sar-Met-SP/TDAG8 mice, then treated with 0.125% collagenase IA (Sigma) and 0.25% trypsin (Sigma). DRG neurons were grown on coverslips for 12 h before calcium or sodium imaging.

METHOD DETAILS

Preparation of agents and drugs

[Sar9,Met(O2)11]-SP (Sar-Met-SP) (NK1 receptor agonist), RP67580 (NK1 receptor antagonist, (3aR,7aR)-Octahydro-2-[1-imino-2-(2-methoxyphenyl)ethyl]-7,7-diphenyl-4H-isoindol), H89 dihydrochloride (PKA inhibitor, N-[2-[[3-(4-Bromophenyl)-2-propenyl]amino]ethyl]-5-isoquinolinesulfinamide dihydrochloride), and tetrodotoxin (TTX, TTX-sensitive voltage-gated sodium channel blocker), Psalmotoxin (PcTx1, ASIC1a blocker), and Capsazepine (TRPV1 blocker) were from Torcis Bioscience (Bristol, UK). Clodronate-liposome (Macrophage blocker) was from LIPOSOMA (Amsterdam, The Netherlands). IB4-saporin (IB4-SAP, ablation of IB4-positive neurons) and saporin (SAP) were from ATSbio (Carlsbad, CA, USA). A803467 ($Na_v1.8$ blocker) was from TargetMol (Wellesley Hills, MA, USA). ZD7288 (HCN blocker) and Chemical name:2-(1,3-Dimethyl-2,6-dioxo-1,2,3,6-tetrahydro-7H-purin-7-yl)-N-(4-isopropylphenyl)acetamide (HC030031, TRPA1 blocker) were from MedChemExpress (Monmouth Junction, NJ, USA). 2,2,2 tribromoethanol (Avertin) was from Alfa Aesar (Ward Hill, MA, USA). APETx2 (ASIC3 blocker) was from Alomone Labs (Jerusalem, Israel). DL-Fluorocitric acid (FC, SGC blocker) barium salt, 2-(N-morpholino)ethanesulfonic acid (MES), and 4-(2-hydroxyethyl)-1-piperazineethanesulfonic acid (HEPES) were from Sigma-Aldrich (St. Louis, MO, USA). Synthesis and use of anthra[2,1-c][37,38,44] thiadiazole-6,11-dione (NSC745885, TDAG8 inhibitor) was described in a previous study.[29] For animal experiments, all drugs or compounds were diluted in saline before injection.

Surgery

Chronic constriction injury (CCI) of the sciatic nerve was performed as described.[29] Mice were anesthetized with avertin (0.4–0.6 mg/g, intraperitoneally) and the sciatic nerve of the mid-thigh level on right side was exposed by using surgical scissors. Three snug ligatures of chronic SOFTSILK 3-0 sutures (Taiwan) were loosely tied around the nerve with about 1 mm space between the knots. After ligation, the muscle and skin of the mouse were sutured and disinfected with providone-iodine. Mice were kept warm during surgery and observed after surgery once a day for 1 week. The sham control involved the same procedure but without ligating the nerve.

Drug injection and treatments

Depletion of macrophage

To deplete macrophages, ICR male mice were intraperitoneally injected with 1 mg clodronate-liposomes (clodronate, CLD)[59] weekly from 1 to 4 weeks after CCI. Behavioral tests were performed at 0–14 weeks after CCI. $N = 6$ male mice. Immunostaining for M1 and M2 macrophages was performed at 1 h after the 4th injection of clodronate. $N = 3$ male ICR mice.

Ablation of IB4(+) neurons

ICR mice were intrathecally injected with IB4-saporin (IB4-SAP, 0.06 mg/mL) or SAP (0.06 mg/mL) at 1 week before CCI surgery.[33] Behavioral tests were performed at 0–14 weeks after CCI. At 2 and 14 weeks, DRG were taken and cultured for calcium imaging.

Inhibition of receptors, channels, or enzymes

For inhibitor or blocker experiments, the drug concentration and test time were selected according to the time courses (A803467, tetrodotoxin, ZD7288) or previous studies (H89, FC). ICR mice were intraplantarly (i.pl.) injected with 25 pmol of the $Na_v1.8$ selective blocker A803467 at 1, 2, or 3 weeks after CCI, and behavioral tests were performed at 3 h after injection. ICR mice were i.pl. injected with 125 pmol tetrodotoxin (TTX), TTX-sensitive sodium channel blocker, at 2 or 14 weeks after CCI, and behavioral tests were performed 4 h after injection, according to the time course. ICR mice were i.pl. injected with 1.25 nmol H89, a PKA inhibitor, at 1, 2, 3, 4 or 5 weeks after CCI, and behavioral tests were performed 4 h after injection.[60] For primary culture, H89 was used at 1 μM. ICR mice were i.pl. injected with 2.5 nmol ZD7288, a hyperpolarization-activation cyclic nucleotide-gated ion channel (HCN) inhibitor, at 1, 2, or 3 weeks after CCI, and behavioral tests were performed 2 h after injection.

For primary culture, APETx2 (ASIC3 blocker), PcTx1 (ASIC1a blocker), HC030031 (TRPA1 blocker), and Capsazepine (TRPV1 blocker) were used at 10μM.

SGC inhibition

To inhibit SGC activation or proliferation, ICR mice were intrathecally injected with 1 nmol FC[31] or vehicle control (Ctrl) at week 2 after CCI surgery. Behavioral tests were performed before (0 weeks) or 1–19 weeks after CCI. Immunostaining was performed before CCI (0w) or at 1, 2, 4, 8, 14, or 19 weeks after CCI. Intrathecal injection was performed as follows: the fifth to sixth part of the lumbar spine (near the root of the tail) was disinfected with 75% alcohol. The needle (30 G×1/2 [0.3 mm × 13 mm] plastic needle, BD) in a Hamilton syringer was inserted in the space between the 4th and 5th lumbar spine and 5 to 10 μL drug was injected. If the needle was successfully inserted in the sheath, the tail of the mouse is slightly upturned. After the experiment, the physical condition of the mouse was observed for 12 h.

SP and RP67580 treatments

In SP experiments, 1 nmol Sar-Met-SP[61,62] was delivered to the injured sciatic nerve or 1 nmol RP67580[63,64] was intrathecally administered at week 1 after CCI. Behavioral tests were performed before (0 weeks) or at 1–19 weeks after CCI. H&E staining, immunostaining, and mRNA expression measurement were performed at 2 or 14 weeks after CCI.

Histological staining and immunostaining

Histological staining of the sciatic nerve or DRG was performed as described.[29] Before (0 weeks) or 1, 2, 4, 8, and 14 weeks after CCI surgery, the sciatic nerve from the ipsilateral sides of TDAG8$^{+/+}$, TDAG8$^{-/-}$, vector control (Ctrl), shTDAG8, clodronate-injected (CLD), and Sar-Met-SP/TDAG8$^{-/-}$ mice was excised, fixed in 25% formalin, then in 50% ethanol. Fixed tissues were embedded in paraffin and sectioned with use of a microtome, then stained with hematoxylin and eosin (by the Taiwan Mouse Clinic, Taipei). Some sections were stained with the primary antibody anti-CD80 (1:250, Biorbyt, Cambridge, UK) or anti-CD163 (1:100, Biorbyt) overnight, then with alkaline phosphatase-conjugated anti-rabbit IgG antibody (1:1000, Jackson Immunoresearch, West Grove, PA, USA) for 1 h, followed by signal development with 5-bromo-4-chloro-3-indolyl phosphate/nitro blue tetrazolium (BCIP/NBT, Merck Millipore, Darmstadt, Germany) for 1 h. Immune cells were observed under a light microscope with a 100x objective (Leica DM500, Bensheim, Germany), and the number of cells was counted in a 1-mm^2 region and represented as cell density (cells/mm^2). Each slide contained two sections and 5–6 regions were selected for each section. Three mice were used for all time points.

Staining of SGCs was as described.[65] In brief, L5 DRG tissues were excised before (0 weeks) or 1, 2, 4, 8, 14 weeks after CCI surgery from TDAG8$^{+/+}$ and TDAG8$^{-/-}$ mice, 2 and 19 weeks after CCI from control or FC-injected mice, and 2 and 14 weeks after CCI from RP67580/TDAG8$^{-/-}$ mice. DRG were frozen in freezing solution and cut at 12-μm thick by using a cryostat (Leica microsystem 3510S, Bensheim, Germany). Sections were co-stained with the primary antibodies anti-peripherin (PERI, 1:500, Sigma) and anti-glial fibrillary acidic protein (GFAP; 1:1000; Dako, Santa Clara, CA, USA), followed by TRITC-conjugated goat anti-mouse IgG antibody (1:250, Sigma) and FITC-conjugated goat anti-rabbit-IgG antibody (1:250, Sigma). Cell images were observed under a fluorescence microscope with a 63x objective (Leica DMI3000B, Germany). The digitized images were captured by using MetaVue. PERI-positive neurons surrounded by GFAP-positive SGCs in one-third or more of the PERI circumference were counted (GFAP+) and expressed as a percentage of total PERI-immunoreactive (IR) neurons (PERI+) in the fields analyzed. Data for each treatment group were collected from 7 to 13 slides, and each slide contained more than 8 DRG sections. N = 3 for each treatment group.

For immunostaining of TDAG8 and other DRG neuron markers, L4, 5 DRG tissues were excised before (0 weeks) or at 2, 14 weeks after CCI surgery. Sections were co-stained with the primary antibodies anti-TDAG8 (1:100, Genesis, Dai et al., 2017) and anti-neurofilment (N52, 1:500, Sigma); anti-TDAG8 and isolectin B4-FITC (IB4, 1:250, Sigma); anti-TDAG8 and anti-calcitonin gene related peptide (CGRP, 1:100, Santa Cruz); anti-TDAG8 and anti-fatty acid binding protein 7 (FABP7, 1:100, Proteintech).

Behavioral tests

Pain behavioral tests were performed as described.[9] Briefly, mice ($n \geq 6$ per group) were pre-trained for 1 to 2 h each day for 2 days before the test. To assess mechanical nociceptive responses, a series of von Frey fibers (0.16, 0.4, 0.6, 1.0, 1.4, 2.0, 4.0 g, Touch-Test, North Coast Medical, Morgan Hill, CA, USA) were applied in ascending order beginning with the finest fiber. For each paw, a von Frey fiber was applied 5 times at 5-s intervals to the plantar surface of the hind paw at various times after injections and both paws were tested. The paw withdrawal threshold (PWT) was determined when paw withdrawal was observed in more than 3 of 5 applications.

For thermal nociceptive response to radiant heat, the plantar surfaces of mouse both hind paws were stimulated with a light bulb (30% intensity, 251 mW/cm^2). The latency to paw withdrawal (PWL) from radiant heat was measured. Measurements from 3 trials at 1-min intervals for each paw were averaged.

Measurement of cAMP and cytokines

Extraction of intracellular cAMP was performed as described.[23] TDAG8$^{+/+}$ and TDAG8$^{-/-}$ mice were sacrificed before (0 weeks) or after (2 or 14 weeks) CCI surgery. Sciatic nerves or L4-6 DRG were taken and flash-frozen in liquid nitrogen and ground to a fine powder under liquid nitrogen, then 0.1 M HCl (10-fold volume of frozen tissue) was added. After centrifugation at 600 ×g for 10 min to remove debris, the

supernatant was directly used in the assay or frozen for later analysis. The lysates were dried, and cAMP level in dried lysates was quantified by use of a cAMP immunoassay kit (R&D systems, Ann Arbor, MI, USA) according to the manufacturer's protocol. For cytokine analysis, tumor necrosis factor α (TNF-α) (#MTA00B), interleukin 6 (IL-6) (#M6000B) or interleukin 10 (IL-10) (#M1000B) were measured with ELISA kits from R&D system (Minnesota, USA) as instructed.

Imaging of intracellular Ca^{2+} ($[Ca^{2+}]_i$) or Na^+ ($[Na^+]_i$) level

$[Ca^{2+}]_i$ imaging was performed as described.[48] DRG neurons were pre-incubated at 37°C with 1.3 μM Fura-2-acetoxymethyl ester (Fura-2-AM, calcium dye, Thermo Fisher Scientific) or SBFI (sodium dye) in HEPES/MES buffer (125 mM NaCl, 1 mM KCl, 5 mM $CaCl_2$, 1 mM $MgCl_2$, 8 mM glucose, 10 mM HEPES and 15 mM MES, pH 7.6). After being washed, cells were supplemented with HEPES/MES buffer (pH 7.6), then stimulated with HEPES/MES buffer (pH 6.8). The pH-evoked Ca^{2+} transients were recorded by use of a Ca^{2+} imaging system equipped with a Leica DMI3000B fluorescence microscope and analyzed by use of MetaFluor software. After recording, DRG neurons were stained with 0.7 mg/mL IB4-FITC (Sigma) for 5 min to label IB4(+) neurons, then observed under a fluorescence microscope (Leica DMI3000B) equipped with MetaView software.

For $[Na^+]_i$ imaging, similar procedures were performed, except using Na^+ dye, SBFI (Thermo Fisher Scientific).

RNA preparation and quantitative RT-PCR

DRG RNA extraction was performed as described.[23] Each DRG pool contained at least 9–12 L4-L6 DRG from 3 to 4 mice or at least 4–6 L5 DRG from 4 to 6 mice. RNA was extracted by using the RNeasy kit (Qiagen, Valencia, CA). The gene primers (100 nM), derived cDNA, and master mix (SYBR green I and AmpliTaq Gold DNA polymerase [Applied Biosystems, Foster City, CA]) were mixed for PCR reactions and product detection by using ABI Prism 7300. The thermal cycling conditions were 95°C for 10 min, followed by 40 cycles of 95°C for 15 s, and 60°C for 1 min. The threshold cycle (Ct) values of both the targets and internal reference (mGAPDH) were measured from the same samples, and target gene expression relative to that of mGAPDH was calculated by the comparative Ct method. For each time point, 2–3 preparations were run in triplicate or quadruplicate. All data were combined for statistical analysis.

The primer sequences were 5′-atagtcagcgtcccagccacc (forward)/5′-cgcttcctttgcacaaggtg (reverse) for TDAG8 (197 bp); 5′-tttcacctg tcttggctcct (forward)/5′-caggatagtggtggggattg (reverse) for ASIC3 (100 bp); 5′-tctccactggtgttgagacg (forward)/5′-gggtctttgaactcgctgtc (reverse) for TRPV1 (151 bp); 5′-caacgcactcataggagcaa (forward)/5′-cttgccagcaaacagattgac (reverse) for $Na_v1.7$ (106 bp); 5′-gtagtggtg-gatgccttggt (forward)/5′-aagtggccggtattgttttg (reverse) for $Na_v1.8$ (217 bp); and 5′-ggagccaaacgggtcatcatctc (forward)/5′-gaggggccatcca-cagtcttct (reverse) for GAPDH (233 bp), as an internal control.

QUANTIFICATION AND STATISTICAL ANALYSIS

All data are presented as mean ± SEM. For behavioral tests, gene expression, cAMP analysis, calcium and sodium signals, and immune cell density, unpaired t tests, one- or two-way ANOVA with post-hoc Bonferroni test were used to compare results for multiple groups. For analysis of calcium or sodium signals and immune cell density, Mann-Whitney U test was used. For estimating population proportion, the z-test was used to test the level of significance, with 95% confidence intervals for proportions estimated from Biometrika tables for statisticians.[66] $p < 0.05$ was considered statistically significant. A statistical power analysis was performed for sample size estimation, based on data from the pilot study. The effect size for t test was 3.4 and for two-way ANOVA was 0.30. Given $\alpha = 0.05$, power = 0.8, the sample size was N = 3/group mice for t test or total N = 48 mice for two-way ANOVA (G*Power 3.1). Our sample size of $N \geq 3$ or total $N \geq 48$ was adequate.